A Transcriptional switch point during hematopoietic stem and progenitor cell ontogeny

Citation for published version:
Sugiyama, D, Joshi, A, Kulkeaw, K, Tan, KS, Yokoo-Inoue, T, Mizuochi-Yanagi, C, Yasuda, K, Doi, A, Iino, T, Itoh, M, Nagao-Sato, S, Tani, K, Akashi, K, Hayashizaki, Y, Suzuki, H, Kawaji, H, Carninci, P & Forrest, ARR 2017, 'A Transcriptional switch point during hematopoietic stem and progenitor cell ontogeny', *Stem Cells and Development*, vol. 26, no. 5, pp. 314-327. https://doi.org/10.1089/scd.2016.0194

Digital Object Identifier (DOI):
10.1089/scd.2016.0194

Published In:
Stem Cells and Development

Stem Cells and Development
© Mary Ann Liebert, Inc.
DOI: 10.1089/scd.2016.0194

Title: A Transcriptional switch point during hematopoietic stem and progenitor cell ontogeny

Daisuke Sugiyama[1,2,3,*,¶], Anagha Joshi[4,¶], Kasem Kulkeaw[1], Keai Sinn Tan[1], Tomoko Yokoo-Inoue[1], Chiyo Mizuochi-Yanagi[1], Kaori Yasuda[5], Atsushi Doi[5], Tadafumi Iino[3], Masayoshi Itoh[6,7,8], Sayaka Nagao-Sato[8], the FANTOM consortium, Kenzaburo Tani[9], Koichi Akashi[10], Yoshihide Hayashizaki[7], Harukazu Suzuki[7], Hideya Kawaji[6,7,8], Piero Carninci[6,7,8] and Alistair R. R. Forrest[7]

[¶] contributed equally

[1]Department of Research and Development of Next Generation Medicine, Faculty of Medical Sciences, Kyushu University, Fukuoka 812-8582, Japan.
[2]Center for Clinical and Translational Research, Kyushu University Hospital, Fukuoka 812-8582 Japan.
[3]Department of Clinical Study, Center for Advanced Medical Innovation, Kyushu University, Fukuoka 812-8582 Japan.
[4]The Roslin Institute and Royal (Dick) School of Veterinary Studies, University of Edinburgh, Easter Bush Campus, Midlothian, EH25 8GR, UK.
[5]Cell Innovator Ltd., 6-10-1 Higashi-ku, Fukuoka, 812-8581 Japan
[6]RIKEN Preventive Medicine and Diagnosis Innovation Program, 1-7-22 Suehiro-cho, Tsurumi-ku, Yokohama, 230-0045 Japan.
[7]RIKEN Center for Life Science Technologies, Division of Genomic Technologies, 1-7-22 Suehiroo-cho, Tsurumi-ku, Yokohama, 230-0045 Japan.
[8]RIKEN Yokohama Institute, Omics Science Center, 1-17-22 Suehiro-cho, Tsurumi-ku, Yokohama, Kanagawa 230-0045 Japan
[9]Division of Molecular and Clinical Genetics, Medical Institute of Bioregulation, Kyushu University, 3-1-1, Maidashi, Higashi-ku, Fukuoka 812-8582, Japan.
[10]Department of Medicine and Biosystemic Science, Kyushu University Graduate School of Medical Sciences, 3-1-1 Maidashi, Higashi-ku, Fukuoka, 812-8582, Japan.

*To whom correspondence should be addressed.
Tel: +81-92-642-6146/6210;Fax: +81-92-642-6146; E-mail: ds-mons@yb3.so-net.ne.jp

Present Address: [Daisuke Sugiyama], MD, PhD
Department of Clinical Study, Center for Advanced Medical Innovation, Kyushu University, Fukuoka 812-8582 Japan.
Station for Collaborative Research1 4F
3-1-1 Maidashi, Higashi-Ku, Fukuoka 812-8582 Japan

Authorship Contributions

D.S.: conception and design, provision of study material and patients, manuscript writing and final approval of manuscript; A.J.: data analysis and interpretation and manuscript writing; K.K., K.S.T and C.M.Y.: provision of study material; K.Y. and A.D.: data analysis and interpretation; T.I., K.T. and K.A.: provision of study material; M.I., S.N.S., Y.H., H.S., H.K., P.C. and A.J.: collection and/or assembly of data and data analysis and interpretation; FANTOM consortium: administrative support.

Abstract

During mammalian embryogenesis, hematopoietic stem and progenitor cells (HSPCs) originate from mesoderm-derived endothelial cells in the aorta-gonad-mesonephros (AGM) region and placenta. Later, HSPCs expand in fetal liver and migrate to bone marrow shortly before birth. Understanding global transcriptional regulation governing HSPC emergence from embryonic stem/induced pluripotent stem cells is necessary to devise clinical applications, such as novel transplantation approaches. Here, to assess transcriptional dynamics during development, we performed cap analysis of gene expression (CAGE) on 10 developmental murine HSPC populations isolated from the AGM region, placenta, fetal liver and bone marrow and identified 15,681 transcripts across HSPC ontogeny. We performed microarray analysis of AGM-derived HSPCs at 9.5 and 10.5 dpc and identified 40 differentially-expressed genes, 23 confirmed as significantly changed by real-time PCR. We conclude that a transcriptional switch point occurs in HSPC ontogeny between 9.5 and 10.5 dpc in the AGM region.

Keywords: hematopoietic stem and progenitor cells, ontogeny, cap analysis of gene expression

Introduction

Hematopoietic stem cells (HSCs) either self-renew or differentiate into all blood cell types. How HSCs maintain a balance between self-renewal and differentiation capacity throughout their lifespan is a key area of investigation [1]. During mammalian embryogenesis, HSCs emerge through a complex process involving ontogenesis at distinct anatomical sites including the yolk sac, the aorta-gonad-mesonephros (AGM) region, placenta (PL) and fetal liver (FL), culminating at birth in colonization of bone marrow (BM) [2]. Understanding molecular mechanisms regulating these steps could have direct clinical applications for HSC transplantation therapy. Decades of research investigating HSC developmental stages and biology demonstrate that intrinsic signals and niche factors regulate these transcriptional programs [3-5], but the genome-wide picture of the transcriptional network governing HSC development and maturation remained far from complete.

In combination with sensitive, well-defined assays based on microarray technology, RNA sequencing and serial analysis of gene expression (SAGE), researchers previously defined transcriptional control mechanisms regulating transient hematopoietic stem and progenitor cell (HSPC) populations [6,7]. However, difficulty in obtaining sufficient amounts of nucleic acid material for subsequent analysis has limited research progress. In addition, researchers found it challenging to compare lists of differentially-regulated genes due to use of different cell populations or HSC classification criteria.

Cap analysis of gene expression (CAGE) sequencing is a method used to identify the 5'ends of capped RNAs based on cap-trapping and hence provides a means to detect likely promoter regions [8]. Here, as part of the FANTOM5 project [9-11], we utilized CAGE sequencing to examine primary murine HSPCs derived from ten spatially-or temporally-critical locations during HSPC development, including the para-aortic-splanchnopleural (p-Sp) region at 8.5 dpc; AGM region at 9.5, 10.5 and 11.5 dpc; PL at 11.5 dpc; FL at 12.5, 14.5 and 19.5 dpc; and BM at 2 to 3-months-old and at 2-years-old. Genome-wide expression profiles of HSPC samples generated from single-molecule CAGE sequencing [12] revealed 15,681 transcription start sites (TSSs). The ten groups were clustered as pre-HSPCs, definitive HSPCs, fetal HSPCs and adult HSPCs, allowing further generation of signature gene lists for each stage. The 15,681 TSSs mapped to 10,385 genes, highlighting an abundance of alternate transcripts and indicating that major changes in the transcriptome

occur in the AGM region from 9.5 to 10.5 dpc. Due to the requirement for a large number of embryos for CAGE sequencing, we performed microarray and real-time PCR analysis in order to confirm the CAGE sequencing data. In consistent with the CAGE sequencing, microarray and real-time PCR confirmed that a transcriptional switch point exists in HSPC ontogeny from 9.5 to 10.5 dpc at the AGM region. This work is part of the FANTOM5 project [9-11]. Data download, genomic tools and co-published manuscripts are summarized at http://fantom.gsc.riken.jp/5/.

Materials and Methods

Animals

ICR and C57BL/6J mice were purchased from Nihon SLC (Hamamatsu, Japan) and Kyudo (Tosu, Japan), respectively. Noon of the day of the plug was defined as 0.5 day post-coitum (dpc). Embryos at various developmental stages were dissected in PBS under a stereomicroscope and the number of somite pairs (SP) counted[13,14]. Animals were handled according to Guidelines for Laboratory Animals of Kyushu University. This study was approved by the Animal Care and Use Committee, Kyushu University (Approval ID: A21-068-0).

Cell preparation

The caudal portion of embryos containing the p-Sp/AGM region was used to obtain a single cell suspension. ICR embryos were used at 8.5 dpc, whereas C57BL/6J embryos were used at 9.5, 10.5 and 11.5 dpc. Single cells were prepared from p-Sp/AGM at 8.5 dpc and the AGM region at 9.5, 10.5 and 11.5 dpc by collagenase treatment (see Supplementary Methods). PLs at 11.5 dpc without deciduas and umbilical vessels were passed through 21-gauge needles and incubated with collagenase. To isolate mononuclear cells, density gradient centrifugation using Lympholyte®-M Cell Separation Media (Cedarlane Laboratories, Ontario, Canada) was performed according to the manufacturer's instructions.

To obtain FL HSPCs, FL cells from 12.5, 14.5 and 19.5 dpc C57BL/6J embryos were filtered through 40-µm nylon mesh (BD Biosciences) and washed once with PBS. Mononuclear cells were isolated as stated above. Mature blood cells were removed by cell

sorting after staining with biotin-conjugated anti-lineage markers (see Supplementary Methods).

To obtain adult BM HSPCs, femurs, tibias and humeri of 2 to 3-month- and 2-year-old C57BL/6J mice were dissected out. BM cells were harvested by flushing with PBS and passed through 40-µm nylon cell strainers (BD Biosciences). Mononuclear cells were isolated and mature blood cells removed by magnetic-activated cell sorting. Cells were incubated with biotin-conjugated antibody as described above. Cells were then incubated with anti-Biotin MicroBeads (MiltenyiBiotec, BergischGladbach, Germany) and passed through MACS® Separation Columns (MiltenyiBiotec).

Flow cytometry and cell sorting

Antibodies used for cell sorting are shown in Supplementary Methods. After gating for propidium-iodide (PI)-negative (living) cells, mesodermal cells, pre-HSPCs and HSPCs were isolated from hematopoietic organs using the following protocol. For the 8.5 dpc p-Sp sample, among E-cadherin-negative non-endodermal cells, mesodermal cells expressing Flk-1 (Vegf receptor 2) and c-Kit (stem cell factor receptor) were sorted out. For the 9.5 dpc AGM region sample, cells double-positive for CD31 (PECAM-1) and CD34 (mucin-like glycoprotein), which include both HSPCs and vascular endothelial cells, were selected. Among CD31+/CD34+ cells, hematopoietic cells expressing c-Kit were sorted out as pre-HSPCs. For the 10.5 dpc AGM region, cells double-positive for CD31 and CD34, which include both HSPCs and vascular endothelial cells, were selected. Among CD31+/CD34+ cells, c-Kit+ hematopoietic cells were sorted. To remove macrophages among hematopoietic cells, we used glycoprotein F4/80. In addition to the AGM region, PL reportedly generates adult repopulating HSCs. Thus we collected a sample from PL expressing c-Kit, CD31 and CD34 at 11.5 dpc [15]. For 12.5 dpc FL [16], we sorted HSPCs expressing Sca1 (stem cell antigen 1), c-Kit and CD45. The common leukocyte marker, CD45 was used as an HSC maturation marker. To remove differentiated cells in 14.5 dpc FL [16], we used Ter119 (erythroid cells), CD45 (leukocytes), CD19 (B-lymphocytes), CD4, CD8 (T-lymphocytes), Gr-1 (granulocytes) and F4/80 (macrophages) markers for cell sorting, and all negative cells were classified as lineage negative (Lin−). Among Lin−/Sca1+ cells, c-Kit+/CD45+ cells were sorted as HSPCs. To examine the effect of aging, BM HSPCs from 2 to 3-month-old or 2-year-old mice were collected by selecting CD34−/Sca1+/c-Kit+ cell populations. Among

Lin−/Sca1+ cells in 2- to 3-month-old BM, c-Kit+ cells were sorted out, regardless of CD34 expression.

RNA extraction and CAGE analysis

Total RNA was isolated and treated with DNase I by using an RNeasy® Plus Micro Kit (Qiagen, Hilden, Germany) according to the manufacturer's instruction. CAGE analysis was carried out as part of the Functional Annotation of the Mammalian Genome 5 (FANTOM5) project at the RIKEN Omics Science Center in Yokohama, Japan.

For real-time PCR, total RNA was isolated and treated with DNase I using an RNAqueous®-4PCR kit (Ambion Inc., Austin, Texas), according to manufacturer's instruction. DNase I-treated RNA was quantitated by NanoDrop 2000/2000c (Thermo Scientific, Delaware). cDNA was prepared using a High Capacity RNA-to-cDNA kit (Life Technologies, Carlsbad, CA) according to the manufacturer's instruction. Briefly, the cDNA synthesis reaction included random octamers, dNTPs, an RNase inhibitor, MuLV reverse transcriptase and DNase I-treated RNA. cDNA was synthesized at 37°C for 60 min followed by denaturation at 95°C for 5 min and holding at 4°C until use.

CAGE bioinformatics analysis

TSSs were assigned to known genes by the FANTOM5 consortium. If the CAGE peak was within 500 bases of the 5' end of a known transcript, it was annotated with the gene name from which that transcript was derived. Enrichment of differentially expressed genes with respect to transcription factor ChIP-seq datasets was calculated using the GSCA tool [17], while functional and pathway enrichment was calculated using Database for Annotation, Visualization and Integrated Discovery (DAVID) [18,19]. ChIP-sequencing data for multiple transcription factors in HSCs and HPCs was collected from gene expression omnibus [10,20-22]. Enrichment for known sequence motifs was performed using HOMER [23]. Genome-wide chromatin modifications in murine HSC samples were downloaded from Mouse ENCODE [19], and methylation data was downloaded from Hogart *et. al* [24]. The SeqMINER tool was used to cluster epigenetic marks [18]. P-values were calculated using a hyper-geometric test. Data analysis was done using a combination of R, perl and shell scripts.

To provide a snapshot of global transcription (the transcriptome) in HSCs across different times and locations, GEDI (Gene expression dynamics inspector) plots (maps) were generated using GEDI23 software (http://www.childrenshospital.org/research/ingber/GEDI/gedihome.htm).

Microarray analysis

Microarray analysis of three independent samples each of AGM-derived HSPCs at 9.5 and 10.5 dpc was performed and compared. Total RNA was isolated from sorted hematopoietic cells using an RNAqueous® Total RNA Isolation Kit (Thermo Fisher Scientific Inc. MA). Total RNA was linearly amplified in two rounds of T7 *in vitro* transcription to generate antisense amplified RNA (aRNA) using a MessageAmp™ II aRNA Amplification Kit (Thermo Fisher Scientific Inc., MA), and an Illumina® TotalPrep RNA Amplification Kit (Thermo Fisher Scientific Inc., MA) according to the manufacturer's instructions. During the second round of amplification, aRNA was labelled with biotin16-UTP. aRNA was purified and verified by spectrophotometry. Subsequently, the Illumina Gene Expression system (Illumina, Inc., CA) was used for direct hybridization of labelled aRNA to gene-specific 50-mer oligonucleotide probes attached to microbeads according to the manufacturer's instruction. After hybridization and washing, BeadChips were immobilized with Cy3-streptavidin (GE Healthcare; Buckinghamshire, UK) and scanned using an Illumina BeadArray Reader.

To analyse microarray data and filter criteria**,** raw signal intensities of six samples were normalized using the quantile algorithm with 'lumi' [25] and the 'preprocessCore' library package [26] on Bioconductor software [27]. Probes called by the 'Detection p-value < 0.05' flag in at least one sample were selected. Then, Linear Models for Microarray Analysis (limma) package [28] of Bioconductor software was applied. Differentially expressed genes were shown on a heat map generated by MeV software [29]. Hierarchical clustering (HCL) analysis was used to sort genes. Color coding indicated distance from the median of each row. DAVID was used to investigate gene ontology (GO) categories enriched for function of differentially expressed genes. Genes encoding factors functioning in transcription, either up-regulated or down-regulated, were selected and validated by real-time PCR. Primer sets used are shown in Supplementary Table S1.

Real-Time PCR analysis

Gene expression levels were measured by real-time PCR using Fast SYBR® Green Master Mix (Life Technologies, Carlsbad, CA) and StepOnePlus™ real-time PCR (Life Technologies, Carlsbad, CA). Forward and reverse primers were designed using PrimerExpress® version 3 (Applied Biosystems) and are listed in Supplementary Table S1. Primer specificity was assessed *in silico* using BLAST (Supplementary Table S1). Primer efficiency was calculated from the slope of the calibration curve using five-fold serial dilution of cDNA prepared from whole embryos or whole fetal organ-derived cDNA in real-time PCR. Amplification conditions were an initial denaturation at 95°C for 20 sec, followed by 40 cycles of denaturation at 95°C for 3 sec and annealing and extension at 60°C for 30 sec. To ensure specific amplification, melting curve analysis was evaluated in all analyses and in a negative control lacking cDNA template. Melting curve analysis consisted of denaturation at 95°C for 15 sec and annealing at 60°C for 1 min/cycle, and annealing temperature was increased 0.3°C/cycle until 95°C.All analyses were performed in triplicate wells; mRNA levels were normalized to *Actb* mRNA, and the relative quantity (RQ) of expression was calculated by delta delta Ct method and compared with a reference sample. Differences were statistically evaluated using Student's *t*-test. P-values less than 0.05 indicated a statistically significant difference.

Results

Collection of HSPC samples from murine tissues at different developmental stages

To characterize changes in the HSPC transcriptome during hematopoietic development, we collected 10 samples from diverse murine organs at selected developmental time points (Fig. 1A). Relevant to marker analysis, E-cadherin− Flk-1+ cells represent mesodermal cells [30], and c-Kit marks intra-aortic clusters of the AGM region [13] [31]. Hematopoietic multipotent progenitors in the p-Sp region at 8.0 dpc [32] and Flk-1+ c-Kit+ cells have been observed at p-Sp/ AGM region at 9.5 dpc [33]. Therefore, we collected E-cadherin–/Flk-1+/c-Kit+ mesodermal cells, the ancestors of hematopoietic cells, from the caudal region (p-Sp) of 8.5 dpc embryos. Cells capable of reconstituting neonatal recipients, known as "pre-HSPCs", have been detected in the p-Sp/AGM region at 9.5dpc [34,35], while cells present at 10.5-11.5 dpc acquire the capacity to reconstitute adult recipients and are known "long term-

repopulating HSCs" [36-38]. We obtained both pre-HSPC and HSPC samples from the AGM region by selecting cells expressing the HSPC marker c-Kit and the endothelial markers CD31 and CD34 [39,40].

Among the 10 HSPC populations identified, we observed that HSPCs form a very small proportion of cells from a given niche (Fig. 1B). For the 8.5 dpc p-Sp sample, E-cadherin−/Flk-1+/c-Kit+ cells represented 2.5±0.18% of the population; for the 9.5 dpc AGM region, CD31+/CD34+/c-Kit+ cells represented 0.68±0.32%; and for 10.5 and 11.5 dpc AGM samples, CD31+/CD34+/c-Kit+/F4/80− cells represented 0.12±0.08% and 0.09±0.14%, respectively. For 11.5 dpc PL, CD31+/CD34+/c-Kit+/F4/80− cells represented 0.79±0.67%; for 12.5 dpc FL, Sca-1+/c-Kit+/CD45+ cells represented 0.75±0.12%; and for 14.5 and 19.5 dpc FL, Lin−/Sca-1+/c-Kit+/CD45+ cells represented 6.57±0.95% and 3.95±1.0%, respectively. Finally, for 2 to 3-month-old and 2-year-old BM, Lin−/Sca-1+/c-Kit+ cells represented 0.044±0.009% and 0.14±0.09%, respectively. Surface markers used to sort each sample are shown in Fig. 2A.

CAGE profiling of murine HSPCs identifies stage-specific transcripts

To study genome-wide transcriptional dynamics during HSPC development, we performed single molecule CAGE [12] sequencing of the 10 samples identified. The rarity of HSPCs during early development represents a challenge requiring collection of large numbers of mouse embryos. Thus, we opted not to generate replicates for each population. By generating approximately 250,000 reads per sample, we identified a total of 15,681 distinct TSSs, which were detected (>=10 tags per million) in at least one of 10 samples, with an average of 8,037 TSSs per sample. We then employed GEDI plots [41] to provide a global gene expression overview of each sample. GEDI plot analysis revealed a distinct transcriptome signature in each of the 10 samples (Fig. 2A). More than 3,000 TSSs showed at least a two-fold difference in expression among p-Sp-8.5 dpc-derived mesoderm, AGM-9.5 dpc-derived pre-HSPCs, and AGM-10.5 dpc-derived HSPC samples, whereas approximately 1,000 TSSs were differentially expressed in HSPCs derived from AGM-11.5 dpc, PL-11.5 dpc, FL-12.5 dpc, FL-14.5 dpc, FL-19.5 dpc, 2 to 3-month-old BM, and 2-year-old BM (Fig.

2B). These observations suggest that major transcriptional changes likely occur in the AGM region between 9.5 and 10.5dpc.

Of TSSs, 15,681 were within 500 bases of a known transcript and were thus annotated with the corresponding gene symbol (representing 10,385 separate genes). The remaining 1,681 TSSs were unannotated and may represent novel HSPC-specific transcripts. The ratio of TSSs to genes was greater for transcription factors (TFs), with 1,518 TSSs mapping to 880 transcription factors (ratio 1.7 compared to 1.5 for all genes), suggesting that alternate transcription of TFs contributes to the regulatory complexity of the mammalian genome [42].

To validate this data using an independent source, we collected ChIP sequencing data for five chromatin modifications (H3K27me3, H3K4me3, H3K4me1, H3K79me2 and H3K27Ac) and for CTCF (CCCTC-binding factor) binding in murine HSCs derived from bone marrow [43]. Over the 15,681 TSSs flanking known transcripts, H3K4me3 and H3K79me2 (predictors of transcription initiation) were enriched near CAGE peaks, while H3K4me1, an enhancer signature, and H3K27me3, a signature of inactive promoters, were depleted, supporting the idea that our analysis detects active transcription initiation events (Fig. 2C). All TSSs also overlapped with binding of CTCF binding, which reportedly preferentially binds near promoters [44].

Finally, to confirm the identity of each sample we checked expression profiles of genes encoding HSPC surface markers (Flk-1, c-Kit, CD31, CD34 and Sca-1) and lineage markers (E-cadherin, F4/80, Gr-1, CD4, CD8, Ter119 and CD19) used for cell sorting (Supplementary Fig. S1A). As expected, we detected high *CD34* levels in all samples. *Flk-1* was detected only in AGM samples and was down-regulated in PL, FL and BM-derived populations. Similarly, *Pecam1* (also known as *CD31*) was expressed at low levels in non-AGM samples. Conversely *c-Kit, Sca-1* and *Ptprc* (also known as *CD45*) were more highly expressed in PL, FL and BM-derived populations relative to AGM. We also detected low levels of *Prom1* (also known as CD133), a marker of some early HSPC populations [45], in mesodermal and pre-HSPC samples.

A transcriptional switch point in HSPC ontogeny occurs in AGM between 9.5and 10.5 dpc

Hierarchical clustering of the 10 HSPC populations assigned them to four clusters:1) pre-HSPCs (p-Sp/8.5 dpc and AGM/9.5 dpc), 2) early HSPCs (AGM/10.5 dpc, AGM/11.5 dpc,

PL/11.5 dpc and FL/12.5 dpc), 3) fetal definitive HSPCs (FL/14.5 dpc and FL/19.5 dpc), and 4) adult definitive HSPCs (BM in 2 to 3-month-old mice and BM in 2-year-old mice) (Fig. 3A). Principal component analysis of the 10 samples was in agreement with partitioning of populations into four corresponding groups (Fig. 3B). In short, this analysis suggests that HSPCs are committed in group 1, become mature and prepared to move to FL in group 2, proliferate, differentiate into mature hematopoietic cells and prepare to move to BM in group 3, and settle in BM and become quiescent in group 4.

To understand differences between groups we identified sets of differentially expressed genes and annotated them using functional and pathway enrichment analysis (Fig. 3C). Although 9.5 and 10.5 dpc HSPCs exhibit similar surface markers, they were clustered into pre-HSPCs and early HSPCs, respectively, based on global gene expression patterns. Consistent with this clustering, the transition from endothelial to HSPC phenotype occurs after 9.5 dpc [13]. Therefore, genes related to vascular development are more highly expressed in group 1 (pre-HSPCs) than in group 2 (early HSPCs) (Fig. 3C). In addition, intra-aortic clusters containing embryonic HSPCs in the AGM region at 9.0-10.5 dpc are likely released into circulation in order to home to FL at 10.5-11.5 dpc based on β1-integrin expression [46,47]. We observed up-regulation of genes functioning in trans-endothelial migration in early rather than pre-HSPCs (Fig. 3C; see“2 versus 1_up”), implying that early HSPCs are prepared to home. Hematopoietic genes were up-regulated in HSPCs in groups 2,3,4, suggesting that group 1 pre-HSPCs are not yet committed to an adult HSPC program. Accordingly, *Pecam1* and *Cdh5* (also known as *VE-cadherin*) were down-regulated in groups 2, 3, and 4 relative to group 1, whereas *Itga2b* (also known as *CD41*) was up-regulated in those groups, as expected. Two key regulators, *Ccnd1* (*cyclin D1*) and *Twist1*, were down-regulated in groups 2,3 and 4 relative to group 1. *Twist1* down-regulation suggests that it may act as a master regulator of HSPC generation, while *Ccnd1*down-regulation suggests that proliferative status of group 1 pre-HSPCs changes as development proceeds (Supplementary Fig. S1B).

Identification of transcription factors regulating HSPC ontogeny

To identify stage-specific TFs governing HSPC development and maturation, we randomly selected 43 TFs differentially expressed (based on at least a two-fold expression change) among the 10 samples (Fig. 4A). Of these, 9 (*Sox18, Hmga2, Sox17, Sox7, Peg3,*

Hey1, Sox11, Snai1 and *Fhl2*) were down-regulated during HSPC maturation (Fig. 4A, blue box). Expression of *Sox17, Sox18* and *Sox7* in AGM/9.5 dpc-derived pre-HSPCs suggests that these cells represent either endothelial/hematopoietic cell progenitors or cells in a transition state [13,48]. About a third (11 of 43) of the TFs (*Hes6, Nr2c2, Tob1, Arhgap17, Irf1, Runx1, Cebpa, Nrip1, Maz, Mta1* and *Aes*) (Fig. 4A, red boxes) was differentially expressed between AGM-9.5 dpc and AGM-10.5 dpc.

We reasoned that dynamically expressed gene loci should be enriched for cis-regulatory motifs recognized by these TFs. Most enriched cis-regulatory motifs for known factors obtained using HOMER software [23] (Fig. 4B) were over-represented relative to random background sequences with the same GC content across all samples. They included motifs recognized by key HSPC TFs including ETS, bHLH proteins, JUN, MYB, PU.1 and STAT proteins. The Gfi1b motif was enriched in 11.5 dpc PL but with *p*-value <1e-3, which was lower than the strict cutoff (p = 1e-5). Three motifs, the ISRE (IFN-stimulated response element) [49] and sequences recognized by Cebp and Runx1, showed progressively greater enrichment during HSPC ontogeny (Fig. 4B). The ISRE motif is found in promoters of genes induced by interferon, which activates dormant HSCs [50]. Moreover, *Ifnar2*, a target of INF alpha, was up-regulated in both FL and BM samples (Supplementary Fig. S1B).

Microarray analysis and gene selection and validation

To identify transcription factors that differentially expressed in AGM-derived HSPCs at 9.5 and 10.5 dpc tissues, we selected a total of 370 differentially expressed genes after statistical analysis with limma (Supplementary Table S2). A heat map of these genes is shown (Fig. 5A). We then conducted enrichment analysis of gene function (Enrichment score > 1.3) of 370 genes. Among them (Supplementary Table S2), 257 genes matched with gene identifier of the DAVID, and seven annotation clusters were enriched (Fig. 5B). We selected 40 genes for real-time PCR analysis, and that those genes are shown in Table 1. These 40 genes were normalized intensities based on three independent samples and consisted of 20 up- and 20 down-regulated genes whose sequence information was obtained through the NCBI website and for which primer sets could be designed for real-time PCR. Then real-time PCR analysis was conducted to analyse gene expression in AGM-derived HSPC at 9.5 and 10.5 dpc. Among 20 up-regulated genes, 11 were significantly up-regulated (P< 0.05) at 10.5

dpc relative to 9.5 dpc (Fig. 5C). Among 20 down-regulated genes, 12 were significantly down-regulated ($p < 0.05$) at 10.5dpc relative to 9.5 dpc (Fig. 5D).

Discussion

Genome-wide datasets have been generated to address how transcriptional networks govern numerous biological processes. Though microarray-based expression profiling is widely used for this purpose, the standard array does not provide information relevant to transcript levels. We therefore used CAGE to construct a global picture of the transcriptional landscape regulating HSPC development, including transcript levels. The CAGE shows that a transcriptional switch point occurs between 9.5 and 10.5 dpc in the AGM region.

Due to the rarity of HSPC samples, we could not generate replicates in CAGE. Based on this outcome, in analysing rare samples, CAGE sequencing could be used for screening purposes to predict stage-specific transcripts, while microarray analysis could be useful for statistical evaluation regardless of TSSs.

Others have reported bias in the non-specific guanine at the 5' end of the CAGE tag [51]. However, such bias is unlikely to underlie the large number of novel unannotated TSSs in HSPCs. First, FANTOM5 CAGE tags are longer, which can multimap and more stringent mapping procedure. In addition, the heliscope CAGE protocol does not use PCR, so tags are not amplified. In FANTOM5, the heliscope CAGE protocol generates a much longer CAGE tag (~32 bases or longer) rather than 18-21 bases in FANTOM3, allowing unequivocal unique mapping of most tags. Also, in FANTOM5 a more advanced probabilistic aligner known as Delve is used and only reports uniquely-mapping tags.

We collected 10 developmental murine HSPC populations isolated from the AGM region, PL, FL and BM. Principal component analysis of TSSs defined 4 HSPC groups among 10 samples (Fig. 3). Previously, Daley's group reported microarray analysis of gene expression during HSC ontogeny [52]. They collected embryonic and adult HSC samples from different stages and sites, in addition to ES cell-derived HSCs. Both of our studies demonstrate that HSPC specification occurs from 10.5 to 12.5 dpc, regardless of cellular location. Their study used CD150 as an HSC marker in FL and BM; thus clustering differences between our groups are likely due to cell surface phenotypes used for cell collection. In addition, they evaluated a 9.5 dpc yolk sac sample, whereas we assessed both 8.5 dpc mesoderm and 9.5 dpc AGM samples. Both of our studies suggest that that dynamic gene expression changes occur in HSPCs from 9.5 to 10.5 or 11.5 dpc, as the transition from

endothelial to hematopoietic HSPC phenotypes occurs [13,37], implying that HSPC commitment is programmed by this time point. Based on this data, it is likely that a major transcriptional switch occurs from 9.5 to 10.5 dpc.

To confirm this transcriptional switch, we performed microarray analysis using triplicate samples. Clustering analysis identifying changes in cytoskeletal genes suggests a transition from endothelial to hematopoietic HSPCs, an outcome consistent with prediction of CAGE sequencing and phenotypic changes observed in HSPCs [13]. Based on ratios, p-values and adjusted p-values, we chose 40 differentially expressed genes to validate by real-time PCR. Among them, 23 were significantly altered (either up-regulated or down-regulated), demonstrating of the utility of the dataset. The function of some of these genes remains unclear in hematopoiesis.

Overall, the dataset presented here should foster identification of novel genes involved in HSPC development and further our understanding of HSPC biology. Our work could also suggest novel approaches to culture and manipulate HSPCs *in vitro* or *ex vivo* in future studies.

Acknowledgements

We thank Mss.Yuka Tanaka and Yuka Horio for technical support, Dr. Elise Lamar for critical reading of the manuscript, and the Ministry of Education, Culture, Sports, Science and Technology, the Ministry of Health, Labor and Welfare, and the Japan Society for the Promotion of Sciencefor funding. Keai Sinn Tan is a recipient of a scholarship from the Tokyo Biochemical Research Foundation, Japan, and a MyPhD scholarship from the Ministry of Higher Education (MOHE), Malaysia. Anagha Joshi is a Chancellors Fellow at the University of Edinburgh. Dr. Joshi's lab is supported by strategic funding from the Biotechnology and Biological Sciences Research Council. FANTOM5 analysis was made possible by a Research Grant to the RIKEN Omics Science Center from MEXT to Yoshihide Hayashizaki. Yoshihide Hayashizaki is also a recipient of a Grant for Innovative Cell Biology by Innovative Technology (Cell Innovation Program) from MEXT, Japan. We thank all members of the FANTOM5 consortium for contributing to sample generation and data-set analysis. We also thank GeNAS for data production.

Author Disclosure Statement

No competing financial interests exist.

References

Uncategorized References

1. Seita J and IL Weissman. (2010). Hematopoietic stem cell: self-renewal versus differentiation. Wiley Interdiscip Rev Syst Biol Med 2:640-53.
2. Mikkola HK and SH Orkin. (2006). The journey of developing hematopoietic stem cells. Development 133:3733-44.
3. Sugiyama D, T Inoue-Yokoo, ST Fraser, K Kulkeaw, C Mizuochi and Y Horio. (2011). Embryonic regulation of the mouse hematopoietic niche. ScientificWorldJournal 11:1770-80.
4. Sasaki T, C Mizuochi, Y Horio, K Nakao, K Akashi and D Sugiyama. (2010). Regulation of hematopoietic cell clusters in the placental niche through SCF/Kit signaling in embryonic mouse. Development 137:3941-52.
5. Swain A, T Inoue, KS Tan, Y Nakanishi and D Sugiyama. (2014). Intrinsic and extrinsic regulation of mammalian hematopoiesis in the fetal liver. Histol Histopathol 29:1077-82.
6. Kim YC, Q Wu, J Chen, Z Xuan, YC Jung, MQ Zhang, JD Rowley and SM Wang. (2009). The transcriptome of human CD34+ hematopoietic stem-progenitor cells. Proc Natl Acad Sci U S A 106:8278-83.
7. Wilhelm BT, M Briau, P Austin, A Faubert, G Boucher, P Chagnon, K Hope, S Girard, N Mayotte, JR Landry, J Hebert and G Sauvageau. (2011). RNA-seq analysis of 2 closely related leukemia clones that differ in their self-renewal capacity. Blood 117:e27-38.
8. Lenhard B, A Sandelin and P Carninci. (2012). Metazoan promoters: emerging characteristics and insights into transcriptional regulation. Nat Rev Genet 13:233-45.
9. Andersson R, C Gebhard, I Miguel-Escalada, I Hoof, J Bornholdt, M Boyd, Y Chen, X Zhao, C Schmidl, T Suzuki, E Ntini, E Arner, E Valen, K Li, L Schwarzfischer, D Glatz, J Raithel, B Lilje, N Rapin, FO Bagger, M Jorgensen, PR Andersen, N Bertin, O Rackham, AM Burroughs, JK Baillie, Y Ishizu, Y Shimizu, E Furuhata, S Maeda, Y Negishi, CJ Mungall, TF Meehan, T Lassmann, M Itoh, H Kawaji, N Kondo, J Kawai, A Lennartsson, CO Daub, P Heutink, DA Hume, TH Jensen, H Suzuki, Y Hayashizaki, F Muller, AR Forrest, P Carninci, M Rehli and A Sandelin. (2014). An atlas of active enhancers across human cell types and tissues. Nature 507:455-61.
10. Carninci P and T Kasukawa and S Katayama and J Gough and MC Frith and N Maeda and R Oyama and T Ravasi and B Lenhard and C Wells and R Kodzius and K Shimokawa and VB Bajic and SE Brenner and S Batalov and AR Forrest and M Zavolan and MJ Davis and LG Wilming and V Aidinis and JE Allen and A Ambesi-Impiombato and R Apweiler and RN Aturaliya and TL Bailey and M Bansal and L Baxter and KW Beisel and T Bersano and H Bono and AM Chalk and KP Chiu and V Choudhary and A Christoffels and DR Clutterbuck and ML Crowe and E Dalla and BP Dalrymple and B de Bono and G Della Gatta and D di Bernardo and T Down and P Engstrom and M Fagiolini and G Faulkner and CF Fletcher and T Fukushima and M Furuno and S Futaki and M Gariboldi and P Georgii-Hemming and TR Gingeras and T Gojobori and RE Green and S Gustincich and M Harbers and Y Hayashi and TK Hensch and N Hirokawa and D Hill and L Huminiecki and M Iacono and K Ikeo and A Iwama and T Ishikawa and M Jakt and A Kanapin and M Katoh and Y Kawasawa and J Kelso and H Kitamura and H Kitano and G Kollias and SP Krishnan and A Kruger and SK Kummerfeld and IV Kurochkin and LF Lareau and D Lazarevic and L Lipovich and J Liu and S Liuni and S McWilliam and M Madan Babu and M Madera and L Marchionni and H Matsuda and S Matsuzawa and H Miki and F Mignone and S Miyake and K Morris and S Mottagui-Tabar and N Mulder and N Nakano and H Nakauchi and P Ng and R Nilsson and S Nishiguchi and S Nishikawa and F Nori and O Ohara and Y Okazaki and V Orlando and KC Pang and WJ Pavan and G Pavesi and G Pesole and N Petrovsky and S Piazza and J Reed and JF Reid and BZ Ring and M Ringwald and B Rost and Y

Ruan and SL Salzberg and A Sandelin and C Schneider and C Schonbach and K Sekiguchi and CA Semple and S Seno and L Sessa and Y Sheng and Y Shibata and H Shimada and K Shimada and D Silva and B Sinclair and S Sperling and E Stupka and K Sugiura and R Sultana and Y Takenaka and K Taki and K Tammoja and SL Tan and S Tang and MS Taylor and J Tegner and SA Teichmann and HR Ueda and E van Nimwegen and R Verardo and CL Wei and K Yagi and H Yamanishi and E Zabarovsky and S Zhu and A Zimmer and W Hide and C Bult and SM Grimmond and RD Teasdale and ET Liu and V Brusic and J Quackenbush and C Wahlestedt and JS Mattick and DA Hume and C Kai and D Sasaki and Y Tomaru and S Fukuda and M Kanamori-Katayama and M Suzuki and J Aoki and T Arakawa and J Iida and K Imamura and M Itoh and T Kato and H Kawaji and N Kawagashira and T Kawashima and M Kojima and S Kondo and H Konno and K Nakano and N Ninomiya and T Nishio and M Okada and C Plessy and K Shibata and T Shiraki and S Suzuki and M Tagami and K Waki and A Watahiki and Y Okamura-Oho and H Suzuki and J Kawai and Y Hayashizaki. (2005). The transcriptional landscape of the mammalian genome. Science 309:1559-63.

11. Forrest AR and H Kawaji and M Rehli and JK Baillie and MJ de Hoon and V Haberle and T Lassman and IV Kulakovskiy and M Lizio and M Itoh and R Andersson and CJ Mungall and TF Meehan and S Schmeier and N Bertin and M Jorgensen and E Dimont and E Arner and C Schmidl and U Schaefer and YA Medvedeva and C Plessy and M Vitezic and J Severin and C Semple and Y Ishizu and RS Young and M Francescatto and I Alam and D Albanese and GM Altschuler and T Arakawa and JA Archer and P Arner and M Babina and S Rennie and PJ Balwierz and AG Beckhouse and S Pradhan-Bhatt and JA Blake and A Blumenthal and B Bodega and A Bonetti and J Briggs and F Brombacher and AM Burroughs and A Califano and CV Cannistraci and D Carbajo and Y Chen and M Chierici and Y Ciani and HC Clevers and E Dalla and CA Davis and M Detmar and AD Diehl and T Dohi and F Drablos and AS Edge and M Edinger and K Ekwall and M Endoh and H Enomoto and M Fagiolini and L Fairbairn and H Fang and MC Farach-Carson and GJ Faulkner and AV Favorov and ME Fisher and MC Frith and R Fujita and S Fukuda and C Furlanello and M Furino and J Furusawa and TB Geijtenbeek and AP Gibson and T Gingeras and D Goldowitz and J Gough and S Guhl and R Guler and S Gustincich and TJ Ha and M Hamaguchi and M Hara and M Harbers and J Harshbarger and A Hasegawa and Y Hasegawa and T Hashimoto and M Herlyn and KJ Hitchens and SJ Ho Sui and OM Hofmann and I Hoof and F Hori and L Huminiecki and K Iida and T Ikawa and BR Jankovic and H Jia and A Joshi and G Jurman and B Kaczkowski and C Kai and K Kaida and A Kaiho and K Kajiyama and M Kanamori-Katayama and AS Kasianov and T Kasukawa and S Katayama and S Kato and S Kawaguchi and H Kawamoto and YI Kawamura and T Kawashima and JS Kempfle and TJ Kenna and J Kere and LM Khachigian and T Kitamura and SP Klinken and AJ Knox and M Kojima and S Kojima and N Kondo and H Koseki and S Koyasu and S Krampitz and A Kubosaki and AT Kwon and JF Laros and W Lee and A Lennartsson and K Li and B Lilje and L Lipovich and A Mackay-Sim and R Manabe and JC Mar and B Marchand and A Mathelier and N Mejhert and A Meynert and Y Mizuno and DA de Lima Morais and H Morikawa and M Morimoto and K Moro and E Motakis and H Motohashi and CL Mummery and M Murata and S Nagao-Sato and Y Nakachi and F Nakahara and T Nakamura and Y Nakamura and K Nakazato and E van Nimwegen and N Ninomiya and H Nishiyori and S Noma and S Noma and T Noazaki and S Ogishima and N Ohkura and H Ohimiya and H Ohno and M Ohshima and M Okada-Hatakeyama and Y Okazaki and V Orlando and DA Ovchinnikov and A Pain and R Passier and M Patrikakis and H Persson and S Piazza and JG Prendergast and OJ Rackham and JA Ramilowski and M Rashid and T Ravasi and P Rizzu and M Roncador and S Roy and MB Rye and E Saijyo and A Sajantila and A Saka and S Sakaguchi and M Sakai and H Sato and S Savvi and A Saxena and C Schneider and EA Schultes and GG Schulze-Tanzil and A Schwegmann and T Sengstag and G Sheng and H Shimoji and Y Shimoni and JW Shin and C Simon and D Sugiyama and T Sugiyama and M Suzuki and N Suzuki and RK Swoboda and PA t Hoen and M Tagami and N Takahashi and J Takai and H Tanaka and H

Tatsukawa and Z Tatum and M Thompson and H Toyodo and T Toyoda and E Valen and M van de Wetering and LM van den Berg and R Verado and D Vijayan and IE Vorontsov and WW Wasserman and S Watanabe and CA Wells and LN Winteringham and E Wolvetang and EJ Wood and Y Yamaguchi and M Yamamoto and M Yoneda and Y Yonekura and S Yoshida and SE Zabierowski and PG Zhang and X Zhao and S Zucchelli and KM Summers and H Suzuki and CO Daub and J Kawai and P Heutink and W Hide and TC Freeman and B Lenhard and VB Bajic and MS Taylor and VJ Makeev and A Sandelin and DA Hume and P Carninci and Y Hayashizaki. (2014). A promoter-level mammalian expression atlas. Nature 507:462-70.

12. Kanamori-Katayama M, M Itoh, H Kawaji, T Lassmann, S Katayama, M Kojima, N Bertin, A Kaiho, N Ninomiya, CO Daub, P Carninci, AR Forrest and Y Hayashizaki. (2011). Unamplified cap analysis of gene expression on a single-molecule sequencer. Genome Res 21:1150-9.
13. Mizuochi C, ST Fraser, K Biasch, Y Horio, Y Kikushige, K Tani, K Akashi, M Tavian and D Sugiyama. (2012). Intra-aortic clusters undergo endothelial to hematopoietic phenotypic transition during early embryogenesis. PLoS One 7:e35763.
14. MH K. *The Atlas of Mouse Development*. (1992). Elsevier Academic Press, London.
15. Ottersbach K and E Dzierzak. (2005). The murine placenta contains hematopoietic stem cells within the vascular labyrinth region. Dev Cell 8:377-87.
16. Ema H and H Nakauchi. (2000). Expansion of hematopoietic stem cells in the developing liver of a mouse embryo. Blood 95:2284-8.
17. Joshi A, R Hannah, E Diamanti and B Gottgens. (2013). Gene set control analysis predicts hematopoietic control mechanisms from genome-wide transcription factor binding data. Exp Hematol 41:354-66.e14.
18. Ye T, AR Krebs, MA Choukrallah, C Keime, F Plewniak, I Davidson and L Tora. (2011). seqMINER: an integrated ChIP-seq data interpretation platform. Nucleic Acids Res 39:e35.
19. Huang da W, BT Sherman and RA Lempicki. (2009). Systematic and integrative analysis of large gene lists using DAVID bioinformatics resources. Nat Protoc 4:44-57.
20. Wilson NK, SD Foster, X Wang, K Knezevic, J Schutte, P Kaimakis, PM Chilarska, S Kinston, WH Ouwehand, E Dzierzak, JE Pimanda, MF de Bruijn and B Gottgens. (2010). Combinatorial transcriptional control in blood stem/progenitor cells: genome-wide analysis of ten major transcriptional regulators. Cell Stem Cell 7:532-44.
21. Fan R, S Bonde, P Gao, B Sotomayor, C Chen, T Mouw, N Zavazava and K Tan. (2012). Dynamic HoxB4-regulatory network during embryonic stem cell differentiation to hematopoietic cells. Blood 119:e139-47.
22. Tanaka Y, A Joshi, NK Wilson, S Kinston, S Nishikawa and B Gottgens. (2012). The transcriptional programme controlled by Runx1 during early embryonic blood development. Dev Biol 366:404-19.
23. Heinz S, C Benner, N Spann, E Bertolino, YC Lin, P Laslo, JX Cheng, C Murre, H Singh and CK Glass. (2010). Simple combinations of lineage-determining transcription factors prime cis-regulatory elements required for macrophage and B cell identities. Mol Cell 38:576-89.
24. Hogart A, J Lichtenberg, SS Ajay, S Anderson, EH Margulies and DM Bodine. (2012). Genome-wide DNA methylation profiles in hematopoietic stem and progenitor cells reveal overrepresentation of ETS transcription factor binding sites. Genome Res 22:1407-18.
25. Du P, WA Kibbe and SM Lin. (2008). lumi: a pipeline for processing Illumina microarray. Bioinformatics 24:1547-8.
26. Bolstad BM, RA Irizarry, M Astrand and TP Speed. (2003). A comparison of normalization methods for high density oligonucleotide array data based on variance and bias. Bioinformatics 19:185-93.
27. Gentleman RC, VJ Carey, DM Bates, B Bolstad, M Dettling, S Dudoit, B Ellis, L Gautier, Y Ge, J Gentry, K Hornik, T Hothorn, W Huber, S Iacus, R Irizarry, F Leisch, C Li, M Maechler, AJ Rossini, G Sawitzki, C Smith, G Smyth, L Tierney, JY Yang and J Zhang. (2004). Bioconductor:

open software development for computational biology and bioinformatics. Genome Biol 5:R80.

28. R. Gentleman VC, S. Dudoit, R. Irizarry, W. Huber (eds). (2005). Limma: linear models for microarray data. In: *Bioinformatics and Computa- tional Biology Solutions using R and Bioconductor*. Smyth GK ed. Springer, New York.
29. Saeed AI, V Sharov, J White, J Li, W Liang, N Bhagabati, J Braisted, M Klapa, T Currier, M Thiagarajan, A Sturn, M Snuffin, A Rezantsev, D Popov, A Ryltsov, E Kostukovich, I Borisovsky, Z Liu, A Vinsavich, V Trush and J Quackenbush. (2003). TM4: a free, open-source system for microarray data management and analysis. Biotechniques 34:374-8.
30. Nishikawa SI, S Nishikawa, M Hirashima, N Matsuyoshi and H Kodama. (1998). Progressive lineage analysis by cell sorting and culture identifies FLK1+VE-cadherin+ cells at a diverging point of endothelial and hemopoietic lineages. Development 125:1747-57.
31. Yokomizo T and E Dzierzak. (2010). Three-dimensional cartography of hematopoietic clusters in the vasculature of whole mouse embryos. Development 137:3651-61.
32. Cumano A, JC Ferraz, M Klaine, JP Di Santo and I Godin. (2001). Intraembryonic, but not yolk sac hematopoietic precursors, isolated before circulation, provide long-term multilineage reconstitution. Immunity 15:477-85.
33. Yoshida H, N Takakura, M Hirashima, H Kataoka, K Tsuchida, S Nishikawa and S Nishikawa. (1998). Hematopoietic tissues, as a playground of receptor tyrosine kinases of the PDGF-receptor family. Dev Comp Immunol 22:321-32.
34. Kumano K, S Chiba, A Kunisato, M Sata, T Saito, E Nakagami-Yamaguchi, T Yamaguchi, S Masuda, K Shimizu, T Takahashi, S Ogawa, Y Hamada and H Hirai. (2003). Notch1 but not Notch2 is essential for generating hematopoietic stem cells from endothelial cells. Immunity 18:699-711.
35. Yoder MC, K Hiatt, P Dutt, P Mukherjee, DM Bodine and D Orlic. (1997). Characterization of definitive lymphohematopoietic stem cells in the day 9 murine yolk sac. Immunity 7:335-44.
36. Medvinsky A and E Dzierzak. (1996). Definitive hematopoiesis is autonomously initiated by the AGM region. Cell 86:897-906.
37. Rybtsov S, M Sobiesiak, S Taoudi, C Souilhol, J Senserrich, A Liakhovitskaia, A Ivanovs, J Frampton, S Zhao and A Medvinsky. (2011). Hierarchical organization and early hematopoietic specification of the developing HSC lineage in the AGM region. J Exp Med 208:1305-15.
38. Taoudi S, C Gonneau, K Moore, JM Sheridan, CC Blackburn, E Taylor and A Medvinsky. (2008). Extensive hematopoietic stem cell generation in the AGM region via maturation of VE-cadherin+CD45+ pre-definitive HSCs. Cell Stem Cell 3:99-108.
39. Garcia-Porrero JA, A Manaia, J Jimeno, LL Lasky, F Dieterlen-Lievre and IE Godin. (1998). Antigenic profiles of endothelial and hemopoietic lineages in murine intraembryonic hemogenic sites. Dev Comp Immunol 22:303-19.
40. Fraser ST, M Ogawa, T Yokomizo, Y Ito, S Nishikawa and S Nishikawa. (2003). Putative intermediate precursor between hematogenic endothelial cells and blood cells in the developing embryo. Dev Growth Differ 45:63-75.
41. Eichler GS, S Huang and DE Ingber. (2003). Gene Expression Dynamics Inspector (GEDI): for integrative analysis of expression profiles. Bioinformatics 19:2321-2.
42. Davuluri RV, Y Suzuki, S Sugano, C Plass and TH Huang. (2008). The functional consequences of alternative promoter use in mammalian genomes. Trends Genet 24:167-77.
43. Stamatoyannopoulos JA, M Snyder, R Hardison, B Ren, T Gingeras, DM Gilbert, M Groudine, M Bender, R Kaul, T Canfield, E Giste, A Johnson, M Zhang, G Balasundaram, R Byron, V Roach, PJ Sabo, R Sandstrom, AS Stehling, RE Thurman, SM Weissman, P Cayting, M Hariharan, J Lian, Y Cheng, SG Landt, Z Ma, BJ Wold, J Dekker, GE Crawford, CA Keller, W Wu, C Morrissey, SA Kumar, T Mishra, D Jain, M Byrska-Bishop, D Blankenberg, BR Lajoie, G Jain, A Sanyal, KB Chen, O Denas, J Taylor, GA Blobel, MJ Weiss, M Pimkin, W Deng, GK Marinov,

BA Williams, KI Fisher-Aylor, G Desalvo, A Kiralusha, D Trout, H Amrhein, A Mortazavi, L Edsall, D McCleary, S Kuan, Y Shen, F Yue, Z Ye, CA Davis, C Zaleski, S Jha, C Xue, A Dobin, W Lin, M Fastuca, H Wang, R Guigo, S Djebali, J Lagarde, T Ryba, T Sasaki, VS Malladi, MS Cline, VM Kirkup, K Learned, KR Rosenbloom, WJ Kent, EA Feingold, PJ Good, M Pazin, RF Lowdon and LB Adams. (2012). An encyclopedia of mouse DNA elements (Mouse ENCODE). Genome Biol 13:418.

44. Phillips JE and VG Corces. (2009). CTCF: master weaver of the genome. Cell 137:1194-211.
45. Horn PA, H Tesch, P Staib, D Kube, V Diehl and D Voliotis. (1999). Expression of AC133, a novel hematopoietic precursor antigen, on acute myeloid leukemia cells. Blood 93:1435-7.
46. Hirsch E, A Iglesias, AJ Potocnik, U Hartmann and R Fassler. (1996). Impaired migration but not differentiation of haematopoietic stem cells in the absence of beta1 integrins. Nature 380:171-5.
47. Sugiyama D, K Kulkeaw and C Mizuochi. (2013). TGF-beta-1 up-regulates extra-cellular matrix production in mouse hepatoblasts. Mech Dev 130:195-206.
48. Levy DE, DS Kessler, R Pine, N Reich and JE Darnell, Jr. (1988). Interferon-induced nuclear factors that bind a shared promoter element correlate with positive and negative transcriptional control. Genes Dev 2:383-93.
49. Essers MA, S Offner, WE Blanco-Bose, Z Waibler, U Kalinke, MA Duchosal and A Trumpp. (2009). IFNalpha activates dormant haematopoietic stem cells in vivo. Nature 458:904-8.
50. Joshi A, Y Van de Peer and T Michoel. (2008). Analysis of a Gibbs sampler method for model-based clustering of gene expression data. Bioinformatics 24:176-83.
51. Zhao X, E Valen, BJ Parker and A Sandelin. (2011). Systematic clustering of transcription start site landscapes. PLoS One 6:e23409.
52. McKinney-Freeman S, P Cahan, H Li, SA Lacadie, HT Huang, M Curran, S Loewer, O Naveiras, KL Kathrein, M Konantz, EM Langdon, C Lengerke, LI Zon, JJ Collins and GQ Daley. (2012). The transcriptional landscape of hematopoietic stem cell ontogeny. Cell Stem Cell 11:701-14.
53. Bernt KM, N Zhu, AU Sinha, S Vempati, J Faber, AV Krivtsov, Z Feng, N Punt, A Daigle, L Bullinger, RM Pollock, VM Richon, AL Kung and SA Armstrong. (2011). MLL-rearranged leukemia is dependent on aberrant H3K79 methylation by DOT1L. Cancer Cell 20:66-78.

FIGUE LEGENDS

Figure 1

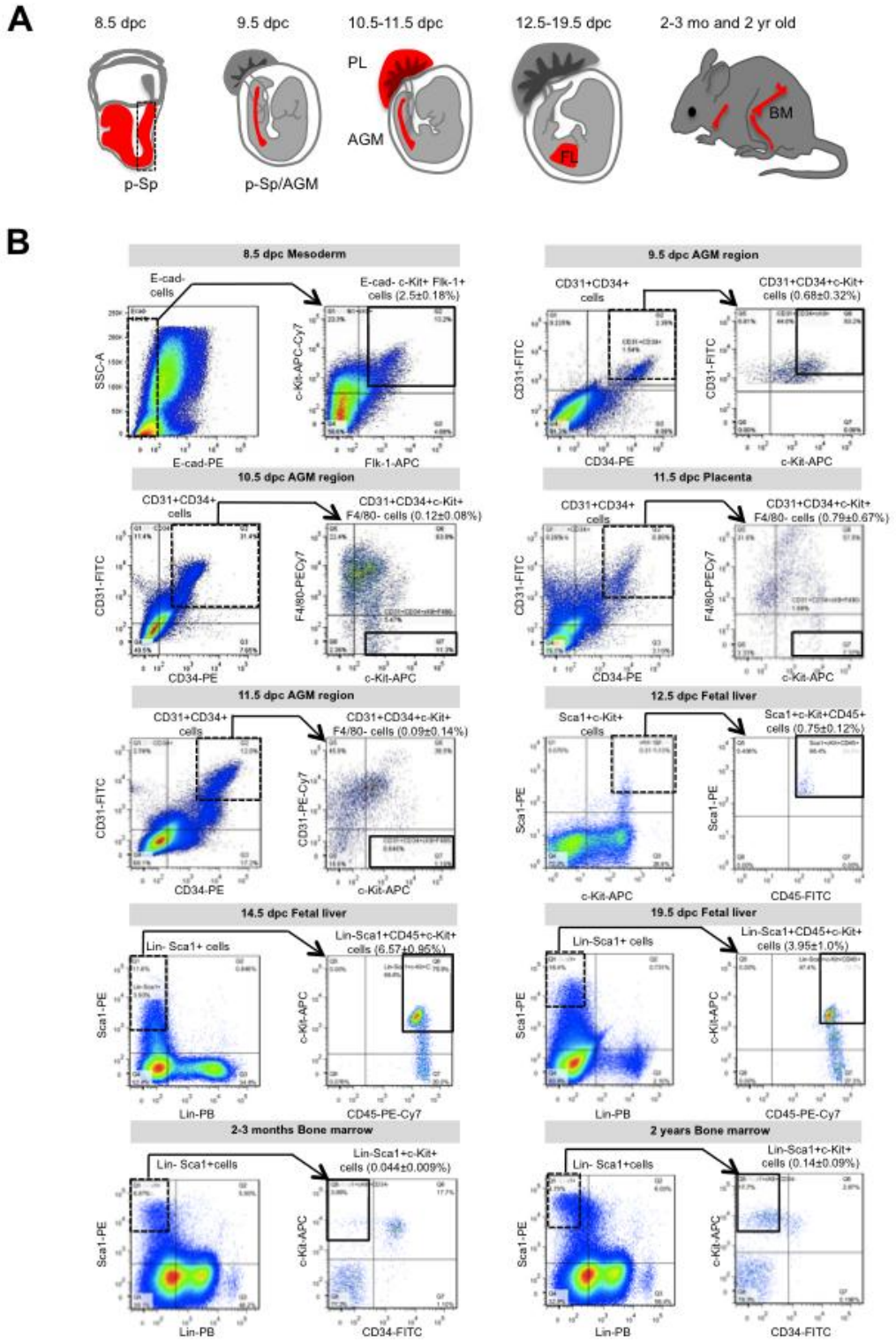

FIG. 1. Isolation of hematopoietic stem and progenitor cells from mouse embryos and adults. **(A)** A total 10 tissues (indicated in red) derived from 9 indicated developmental time points

served as HSPC sources for CAGE analysis. They include:1) caudal regions (p-Sp, dotted line) of 8.5 dpc embryos (mesoderm); 2) 9.5 dpc p-Sp/AGM tissue for pre-HSPCs; 3) AGM tissue at 10.5 dpc and 4) 11.5 dpc; 5) 11.5 dpc placenta (PL); 6) 12.5 dpc fetal liver (FL); 7) 14.5 dpc FL; 8) 19.5 dpc FL; 9) BM from 2 to 3-month (mo)-old mice; and 10) BM from 2-year (yr)-old mice. **(B)** Flow cytometric analysis of hematopoietic tissues based on surface expression of hematopoietic cell markers. Single cell suspensions of indicated embryonic and adult tissues were prepared and analysed by flow cytometry. Isotype control is not shown. To obtain mesodermal cells at 8.5 dpc, E-cadherin-negative cells were gated first. Then among them, Flk-1+ and c-Kit+ cells were analysed. To obtain pre-HSPCs from p-Sp/AGM tissue at 9.5 dpc and HSPCs from AGM tissue at 10.5 dpc and from placenta at 11.5 dpc, CD31+ and CD34+ cells were gated first. Then c-Kit+/F4-80− cells were analysed on CD31+/CD34+ cells. To obtain HSPCs from PL at 11.5 dpc, CD31+ and CD34+ cells were gated first. Then among them, c-Kit+ cells were analysed. To obtain HSPCs from FL at 12.5 dpc, Sca-1+/c-Kit+ cells were gated first and then CD45+ cells were analysed among them. To obtain HSPCs from FL at 14.5 and 16.5 dpc, Lin− and Sca-1+ cells were gated first. Then c-Kit+/CD45+ cells were analysed among them. To obtain HSPCs from BM at 2 to 3-month- and 2 year-old mice, Lin− and Sca-1+ cells were gated first. Then among them, c-Kit+/CD34− cells were analysed.

Figure 2

A

#	Sample	Cellular location	Time	Surface phenotype	# of cells	# of reads	# of TSSs (genes)	GEDI plots
1	p-Sp	p-Sp	8.5 dpc	E-cad-, Flk-1+, c-Kit+	50,549	2.28M	11,454 (8,393)	
2	Pre-HSPCs	AGM	9.5 dpc	CD31+, CD34+, c-Kit+	30,286	0.71M	9,545 (7,095)	
3	HSPCs	AGM	10.5 dpc	CD31+, CD34+, c-Kit+, F4/80-	38,665	0.08M	8,894 (6,879)	
4	HSPCs	AGM	11.5 dpc	CD31+, CD34+, c-Kit+, F4/80-	30,558	0.17M	13,086 (9,227)	
5	HSPCs	PL	11.5 dpc	CD31+, CD34+, c-Kit+, F4/80-	33,379	0.24M	9,951 (7,517)	
6	HSPCs	FL	12.5 dpc	Sca-1+, CD45+,c-Kit+, Lin-	30,357	0.40M	9,796 (7,477)	
7	HSPCs	FL	14.5 dpc	Sca-1+, CD45+,c-Kit+, Lin-	35,758	0.57M	11,810 (8,515)	
8	HSPCs	FL	19.5 dpc	Sca-1+, CD45+,c-Kit+, Lin-	32,139	0.22M	9,420 (7,355)	
9	HSPCs	BM	2-3 mo	CD34-, Sca-1+, c-Kit+, Lin-	55,503	0.47M	11,185 (8,182)	
10	HSPCs	BM	2 yr	CD34-, Sca-1+, c-Kit+, Lin-	66,387	0.25M	11,274 (8,199)	

B

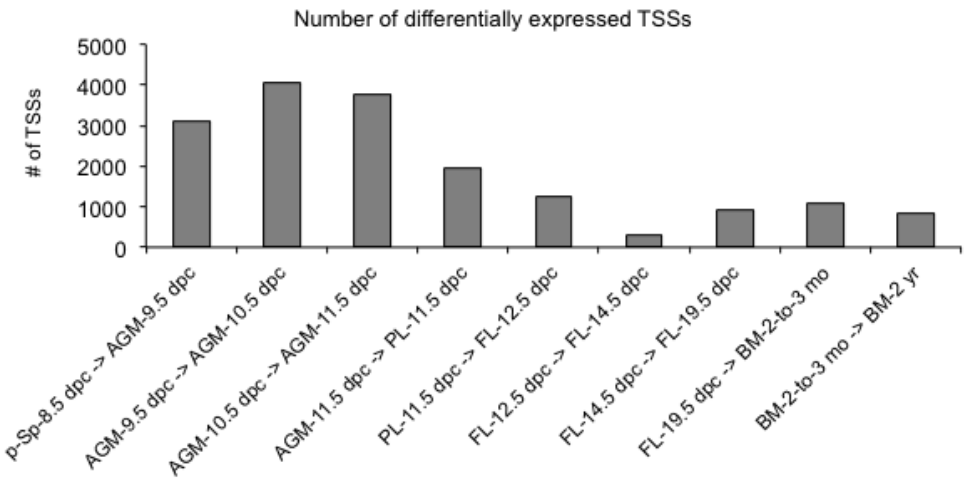

C

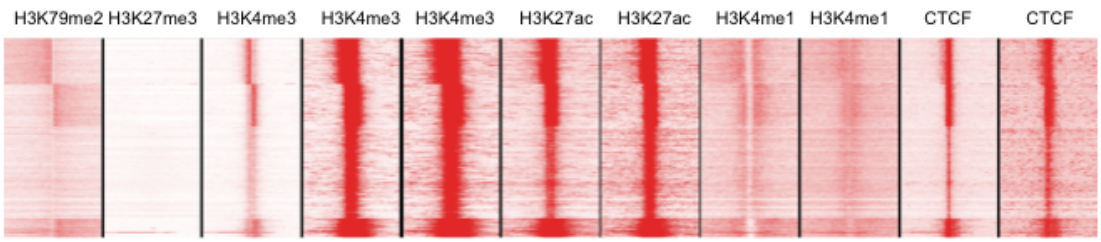

FIG. 2. CAGE analysis over HSPC development. **(A)** Table showing indicated groups depicted in Fig. 1A, with respect to surface phenotypes, number of cells isolated, number of

mapped reads, TSSs identified and total number of genes mapped to for each CAGE sample, as well as GEDI plots of the global transcriptional landscape. Each pixel within a GEDI plot represents a mini-cluster of genes with similar expression pattern across all analysed samples. Pixel color indicates gene expression level for each cluster (blue to red indicates low to high levels, respectively). CAGE libraries were generated and sequenced to an average depth of approximately 250 thousand reads for each sample. Analysis detected use of 15,681 distinct TSSs in 10 samples with an average of ten thousand TSSs in each. **(B)** Number of differentially expressed TSSs between two consecutive stages of HSPC development. Given at least a two-fold difference transcript expression, >3,000 TSSs were differentially expressed between p-Sp-8.5 dpc-derived mesoderm, AGM-9.5 dpc-derived pre-HSPCs and AGM-10.5 dpc-derived HSPCs, whereas ~1,000 TSSs were differentially expressed when comparing AGM-11.5 dpc-, PL-11.5 dpc-, FL-12.5 dpc-, FL-14.5 dpc-, FL-19.5 dpc-, BM-2-to 3-mo, and BM-2 yr-derived HSPCs. **(C)** 15,681 TSSs from all samples were validated using previously published ChIP-sequence data of chromatin modification relevant to HSPCs derived from bone marrow [53]. High levels of H3K4me3 and H3K27ac and lack of H3K4me1 confirmed TSSs as promoter regions. The figure was generated using SeqMINER software.

Figure 3

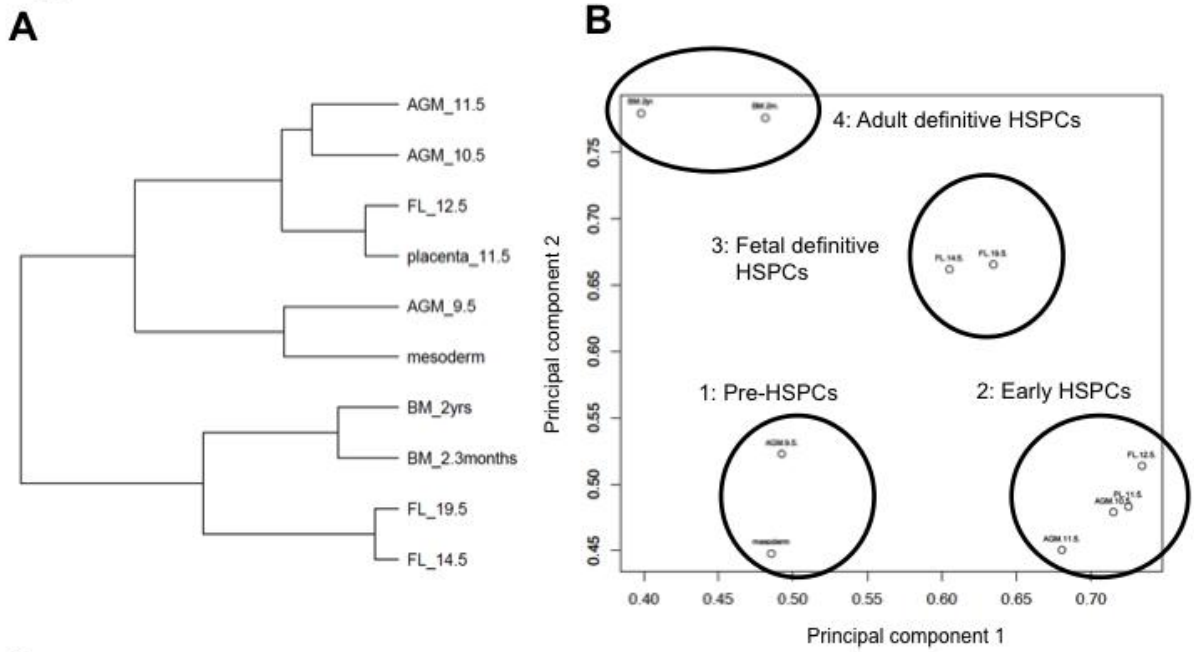

C

Gene set	#	GO enrichment	Pathway enrichment
2 vs 1_down	117	Blood vessel development (2.1e-5) , vasculature development (2.5e-5)	Focal adhesion (9.7e-2)
2 vs 1_up	228	Mitochondrion (2.0e-7)	Fc RI signalling (7.0e-4), leukocyte transendothelial migration (2.0e-2)
2, 3, 4 vs 1_down	409	Blood vessel development (4.6e-10), angiogenesis (1.5e-7)	Focal adhesion (4.5e-6), ECM receptor interaction (3.9e-4)
3, 4 vs 1, 2_down	919	Ribosome (3.8e-41), respiratory chain (5.2e-6)	Huntington's disease (2.5e-21), alzheimer's disease (6.0e-13), parkinson's disease (9.7e-20)
3, 4 vs 1, 2_up	765	Lymphocyte activation (5.0e-15), Haematopoiesis (6.0e-9), Transcription regulation (1.0e-9)	B cell receptor signalling (4.7e-6), MAPK signalling (7.5e-5), Jak-STAT signalling (1.1e-4)
3, 4 vs 2_down	131	Ribosomal protein (1.8e-16)	Ribosome (8.1e-13)
3, 4 vs 2_up	453	Nucleus (2.6e-10), transcription regulation (7.5e-8), haematopoietic organ development (1.3e-2)	MapK signalling (3.6e-3), Notch signalling (3.8e-3), Wnt signalling (1.3e-2)

FIG. 3. Identification of gene signatures indicative of HSPC development. **(A)** Hierarchical clustering of 10 CAGE samples. **(B)** Principal Component Analysis of 10 CAGE samples

showing indicated groups. **(C)** Summary of genes differentially expressed among the four stages, with respective gene ontology (GO) as well as pathway enrichment analysis.

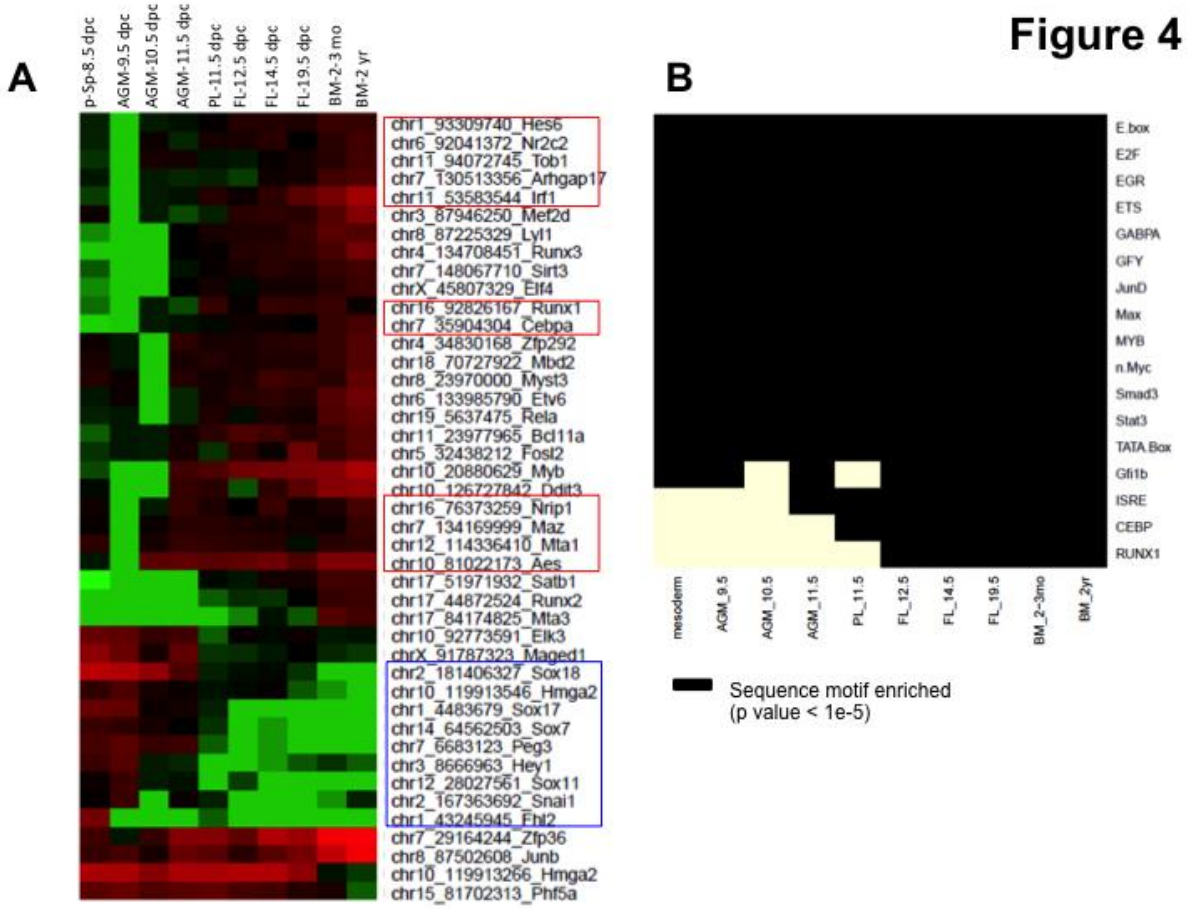

FIG. 4. Changes in global transcription over the course of HSPC ontogeny. **(A)** Heat map showing dynamically expressed transcription factors (TFs) with their TSS location over

HSPC development indicating differential TF expression in the AGM between 8.5and 9.5 dpc. Blue box indicates genes down-regulated during HSPC maturation; red boxes indicate up-regulated genes, including *Hes6*, *Nr2c2*, *Tob1*, *Arhgap17*, *Irf1*, *Runx1*, *Cebpa*, *Nrip1*, *Maz*, *Mta1* and *Aes*. **(B)** Over-represented sequence motifs (black boxes) in each sample. Specifically, *ISRE*, *CEBP* and *Runx1* show dynamic behaviour that reflects a particular pattern during HSPC ontogeny.

Figure 5

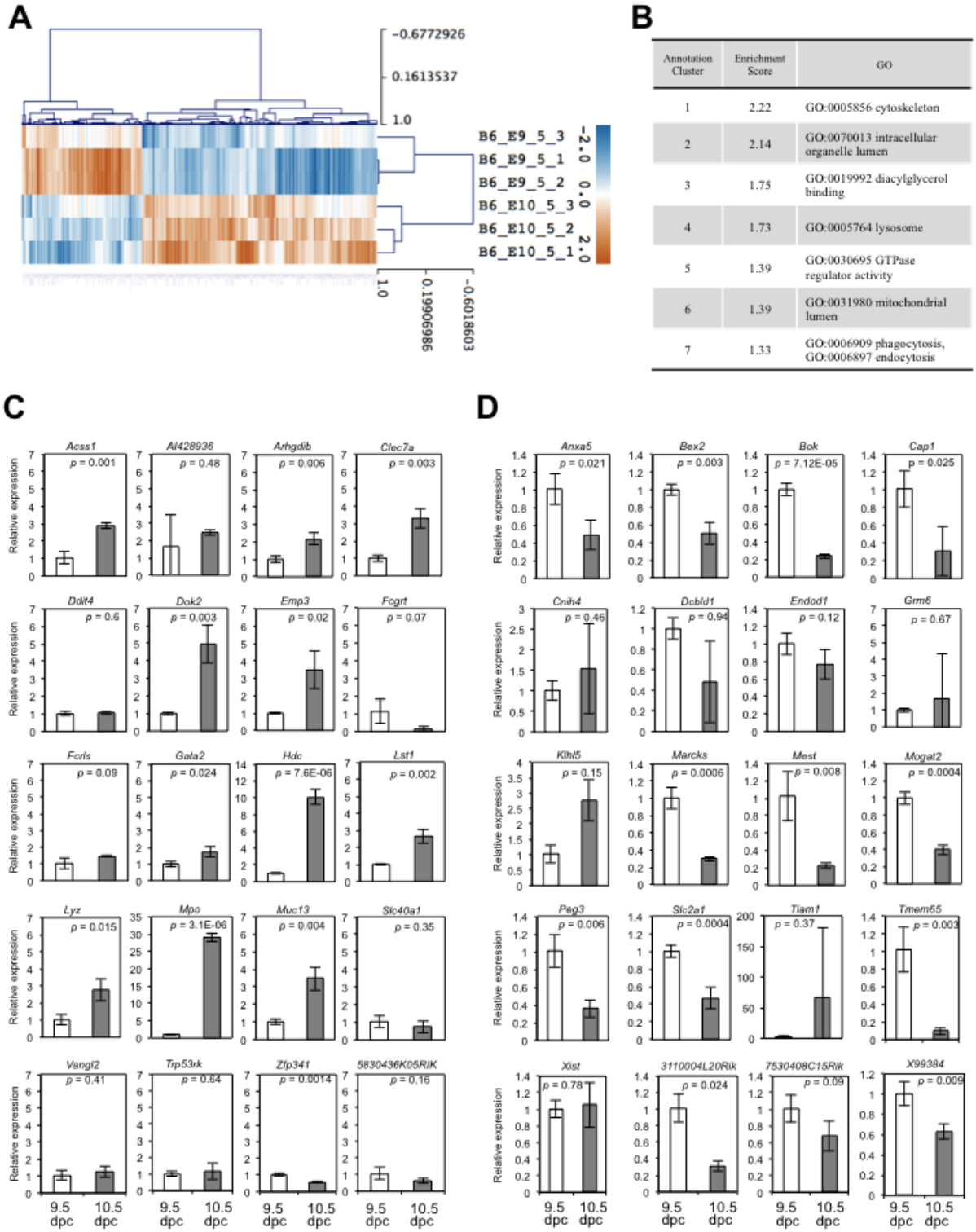

Annotation Cluster	Enrichment Score	GO
1	2.22	GO:0005856 cytoskeleton
2	2.14	GO:0070013 intracellular organelle lumen
3	1.75	GO:0019992 diacylglycerol binding
4	1.73	GO:0005764 lysosome
5	1.39	GO:0030695 GTPase regulator activity
6	1.39	GO:0031980 mitochondrial lumen
7	1.33	GO:0006909 phagocytosis, GO:0006897 endocytosis

FIG. 5. Microarray analysis of AGM-derived HSPCs at 9.5 dpc and 10.5 dpc. Three independent samples of the AGM-derived HSPCs at 9.5 dpc and 10.5 dpc were compared.

(A) Heat map of 370 differentially expressed genes. **(B)** Function enriched (Enrichment Score > 1.3), as indicated by DAVID analysis. Functions of the 257 of 370 genes were annotated into seven clusters: cytoskeleton, intracellular organelle lumen, diacylglycerol binding, lysosome, GTPase regulator activity, mitochondrial lumen and phagocytosis related genes. Based on three independent analyses, genes encoding factors related to transcription (either up-regulated or down-regulated) were selected and validated by real-time PCR. A total of 20 each of up-regulated and down-regulated genes from the microarray were selected and validated by real-time PCR. **(C)** Among up-regulated genes, 11 of 20 showed significant changes ($p < 0.05$) at 10.5 dpc relative to 9.5 dpc in independent samples. **(D)** Among down-regulated genes, 12 of 20 showed significant changes ($p < 0.05$) in the same period in independent samples. Unfilled and grey filled bars represent gene expression levels in AGM-derived HSPCs at 9.5 dpc and 10.5 dpc, respectively. *Actb* served as internal control.

Table1: Differentially-expressed candidate genes.

Forty genes were selected for microarray validation. Shown are normalized intensities in both 9.5 dpc and 10.5 dpc AGM-derived HSCs (n = 3), ratios (non-log fold-change), p-values and adjusted p-values. Up- and down-regulated genes (20 each) sorted by ratio are shown. *Mpo* and *Mest* genes, each ranked by three probes, were counted as one gene.

Probe ID	Symbol	AGM-derived HSCs at 9.5 dpc			AGM-derived HSCs at 10.5 dpc			Ratio	p-value	Adjusted p-value
		Sample#1	Sample#2	Sample#3	Sample#1	Sample#2	Sample#3			
2970324	*Hdc*	830.25	935.83	231.57	9519.32	9364.16	7794.57	15.68899	0.00014	0.07378
4880386	*Muc13*	291.20	293.79	650.28	3445.93	2988.55	2794.07	8.02708	0.00005	0.06115
5720609	*Lyz*	355.62	371.78	610.36	1701.37	2622.91	2588.35	5.23103	0.00007	0.06715
150458	*Trp53rk*	458.18	409.77	277.21	1917.66	2082.78	1026.80	4.28718	0.00041	0.08299
6200719	*Acss1*	410.76	446.32	252.09	1630.10	1529.18	1126.99	3.93188	0.00018	0.07378
4540564	*Dok2*	261.14	265.47	342.33	1220.66	1229.69	881.23	3.81983	0.00003	0.06115
130634	*Ddit4*	568.31	588.80	1092.67	3363.15	2332.50	2439.05	3.74040	0.00042	0.08299
6580021	*Mpo*	3535.14	3506.52	3883.81	9975.33	12586.18	17879.26	3.59923	0.00010	0.07378
2940681	*Gata2*	3451.52	3246.33	4606.56	16151.05	8857.75	13501.76	3.34486	0.00035	0.08299
4060593	*Vangl2*	450.57	481.80	579.40	1761.05	1908.88	1337.61	3.29427	0.00005	0.06115
1450333	*Clec7a*	246.66	231.57	251.49	753.09	821.82	648.83	3.03497	0.00002	0.06115

940541	*Fcrls*	423.85	433.03	326.64	1168.86	1097.15	1270.86	3.00681	0.00004	0.06115
6590167	*Fcgrt*	405.36	404.52	274.40	1159.82	1011.28	975.14	2.94030	0.00013	0.07378
940309	*Mpo*	11146.78	10513.86	11450.52	31002.28	29213.21	31831.42	2.77991	0.00001	0.06115
1010196	*Zfp341*	303.61	315.71	246.30	806.63	856.22	719.41	2.76093	0.00005	0.06115
5860154	*Lst1*	643.90	674.92	767.84	1547.38	2280.48	1888.36	2.71304	0.00013	0.07378
2140221	*Slc40a1*	306.05	313.44	303.61	756.40	692.31	1107.46	2.71045	0.00023	0.07845
6280168	*Mpo*	526.28	528.24	452.79	1190.50	1189.41	1168.86	2.36025	0.00005	0.06115
110717	*AI428936*	333.19	363.03	302.05	815.43	884.37	656.69	2.34904	0.00020	0.07472
1070224	*Emp3*	255.03	263.50	224.43	495.00	657.36	572.78	2.31197	0.00018	0.07378
130661	*5830436K05 RIK*	241.20	253.50	239.45	461.90	569.42	529.51	2.12	0.00016	0.07378
1090180	*Arhgdib*	1187.16	1255.51	1424.35	2509.13	2708.39	2936.27	2.11038	0.00019	0.07378
6660707	*Klhl5*	529.25	557.07	523.35	332.03	242.45	239.44	0.49989	0.00079	0.08614
5270452	*Tiam1*	3596.56	3369.53	2392.86	1724.77	1283.19	1530.37	0.48882	0.00194	0.10631
1500768	*Dcbld1*	881.68	921.93	710.39	342.22	462.24	422.83	0.48747	0.00086	0.08804
1820224	*Marcks*	1643.34	1516.90	1400.90	690.10			0.48363	0.00016	0.07378
4880554	*Cnih4*	2341.05	2386.38	1591.44	872.82	975.52	1036.81	0.46306	0.00098	0.09054
6940068	*X99384*	1487.66	1339.79	1286.74	755.13	501.51	657.07	0.45951	0.00066	0.08413

450372	*Bok*	2243.17	1962.47	2329.19	842.41	945.04	1235.39	0.45776	0.00060	0.08413
6330445	*Mogat2*	698.27	716.26	772.59	307.48	344.58	344.01	0.45521	0.00008	0.07262
3190408	*Mest*	2336.51	2268.08	2692.25	814.69	1242.20	1239.92	0.44471	0.00091	0.09005
3440343	*Cap1*	952.25	998.10	550.70	310.26	330.02	393.64	0.42545	0.00225	0.11264
6350044	*Slc2a1*	7385.06	7320.20	4586.46	2559.53	2795.69	2645.31	0.42422	0.00083	0.08659
3290747	*Bex2*	3216.97	3492.91	2793.40	1537.72	1210.87	1237.43	0.41871	0.00016	0.07378
3990484	*3110004L20 Rik*	1740.60	1768.32	1503.83	638.90	752.33	686.64	0.41	0.00007	0.06715
6450520	*7530408C15 Rik*	4395.28	4543.87	5979.14	2324.44	2188.63	1465.30	0.40	0.00077	0.08610
6770356	*Mest*	7257.15	6954.87	7505.60	2006.52	2951.52	3837.83	0.39148	0.00100	0.09078
6290133	*Endod1*	1245.66	1289.43	950.12	398.92	462.24	488.60	0.38938	0.00015	0.07378
1690019	*Mest*	6712.69	6420.07	6332.16	1794.83	2574.71	3281.06	0.38159	0.00063	0.08413
2480059	*Anxa5*	1860.18	1826.27	1097.72	649.96	544.17	558.57	0.37557	0.00065	0.08413
2690435	*Peg3*	9670.34	9364.16	5634.74	2278.11	2916.39	3233.71	0.34789	0.00069	0.08413
19	*Tmem65*	2148.18	2243.17	1723.06	640.14	658.88	770.88	0.33958	0.00004	0.06115
610092	*Grm6*	1041.87	1021.59	538.14	234.23	245.66	386.25	0.33855	0.00213	0.10902
4060521	*Xist*	2281.13	2399.39	1088.77	471.60	543.83	684.85	0.30890	0.00157	0.10062

Supplemental Data

Supplemental Methods

Embryo staging

Somite pairs (SPs) were counted as a means to stage embryos, as follows [1,2]: 8.5 dpc (5-8 SP), 9.5 dpc (18–22 SP), 10.5 dpc (32-34 SP), and 11.5 dpc (42-46 SP).

Cell preparation

Single cell suspensions were prepared as described with small modifications [2-6]. Tissues representing p-Sp/AGM at 8.5 dpc and the AGM at 9.5, 10.5 and 11.5 dpc were incubated with 1 mg/mL collagenase (Washington Biochem Co., Freehold, New Jersey) in alpha-MEM supplemented with 10% fetal bovine serum for 30 minutes at 37°C, filtered through 40-µm nylon cell strainers (BD Biosciences, San Diego, CA), and washed once in PBS. For 11.5 dpc placenta, placentas without deciduas and umbilical vessels were passed through 21-gauge needles and incubated with 1 mg/mL.

To obtain fetal liver HSPCs at 12.5, 14.5 and 19.5 dpc, mature blood cells were removed. First, mononuclear cells were stained with the following biotin-conjugated antibodies that bind to lineage surface markers of mature blood cells: biotin anti-mouse Ter119 for mature erythrocytes, biotin anti-mouse Ly-6G/Ly-6c (Gr-1) for granulocytes, biotin anti-mouse F4/80 for macrophages, biotin anti-mouse CD45R/B220 for B lymphocytes, and biotin anti-mouse CD4 and biotin anti-mouse CD8 for T lymphocytes. All antibodies were from BioLegend, San Diego, CA. After washing once in PBS, cells were stained with Streptavidin eFluor® 450 (eBioscience, San Diego, CA).

Antibodies for flow cytometry and cell sorting

Antibodies used for cell sorting were: PE-conjugated anti-mouse E-cadherin (R&D Systems, Minneapolis, MN), Alexa Fluor 647 anti-mouse Flk-1 (VEGFR2), APC- and PE-Cy7-conjugated anti-mouse CD117 (c-Kit), Alexa Fluor 488 anti-mouse CD31, PE-conjugated anti-mouse CD34 (eBioscience), PE-Cy7-conjugated anti-mouse F4/80, PE-conjugated anti-mouse Ly-6A/E (Sca-1), PE-Cy7-conjugated anti-mouse CD45, and FITC-conjugated anti-mouse CD34 (eBioscience). Unless otherwise noted, antibodies were from BioLegend. Flow cytometric analysis and cell sorting were carried out using a FACSAria SORP cell sorter (BDIS, San Jose, CA). Data files were analyzed using FlowJo software (Tree Star, Inc., San Carlos, CA).

Supplemental References

1. MH K. *The Atlas of Mouse Development*. (1992). Elsevier Academic Press, London.
2. Mizuochi C, ST Fraser, K Biasch, Y Horio, Y Kikushige, K Tani, K Akashi, M Tavian and D Sugiyama. (2012). Intra-aortic clusters undergo endothelial to hematopoietic phenotypic transition during early embryogenesis. PLoS One 7:e35763.
3. Sasaki T, C Mizuochi, Y Horio, K Nakao, K Akashi and D Sugiyama. (2010). Regulation of hematopoietic cell clusters in the placental niche through SCF/Kit signaling in embryonic mouse. Development 137:3941-52.
4. Sugiyama D, K Kulkeaw and C Mizuochi. (2013). TGF-beta-1 up-regulates extra-cellular matrix production in mouse hepatoblasts. Mech Dev 130:195-206.
5. Sugiyama D, K Kulkeaw, C Mizuochi, Y Horio and S Okayama. (2011). Hepatoblasts comprise a niche for fetal liver erythropoiesis through cytokine production. Biochem Biophys Res Commun 410:301-6.
6. Sugiyama D, M Ogawa, K Nakao, N Osumi, S Nishikawa, S Nishikawa, K Arai, T Nakahata and K Tsuji. (2007). B cell potential can be obtained from pre-circulatory yolk sac, but with low frequency. Dev Biol 301:53-61.

Supplementary Table

Supplementary Table S1. Primers used for real-time PCR.

Gene Symbol	Primer sequence (5'>3')	In *silico* specificity Transcript variant (accession no.)	Amplicon Length (bp)
Muc13	Forward: GGAGAAATGGGCAGAGACAAAG Reverse: TTCGGCAAGCTTCGGTCTT	NM_010739.1	100
Dok2	Forward: CCCACCCTCCTCCTACACTTT Reverse: GACATCTGTGGAAACCCTTTGTC	NM_010071.2	100
Vangl2	Forward: CGGTGACCAATGGGCTTAAG Reverse: GAGAGTTTGAAGAAGGGCACCTT	NM_033509.3	100
Clec7a	Forward: TTGTGCTGAGTCCACTGAATTGTT Reverse: CAGAGGCCAAAGATACTTTAATAAGC	NM_020008.1	101
Fcrls	Forward: TGTGGCGGAGCTTCACTGT Reverse: AAAAGGTGCCGAGGTGTTAGC	NM_030707.3	100
Mpo	Forward: AACCCAGGCGTGTTCAGTAAA Reverse: TCTTCGACACGGTGGTGATG	NM_010824.1	100
Zfp341	Forward: AGCCAGCCCTTGCTTCAGAT Reverse: GTGCTATACGAAGTCCTGTTGCA	NM_199304.1	100
Tmem65	Forward: GCACCGCTTCGAGTCCAT Reverse: AGGTATCGCATTGTGGAAGAATACA	NM_175212.4	103
Lyz	Forward: CTGCCCCTTTCATCTTGCTT Reverse: CCTCCTGAATGCCTCATGACA	NM_013590.2	101
3110004L20Rik	Forward: TCGCTAAGTTCTCCTTACTGGTT Reverse: GTGGAAAACAGCAGCACAGG	NM_001033167.1	101
Mogat2	Forward: GTCTGCCCTGGCACCTACTC Reverse: AGTGACCCCTGCCCTCCTTA	NM_177448.3	102
Hdc	Forward: CAGGGTCTTCGTGATCCACAA Reverse: CACCGTCTCAGCCCCTTCTA	NM_008230.4	100

Acss1	Forward: GGTGGAGCTGAAGAAAATAGTGGAT Reverse: CCCCATGGGAACCTTGGT	NM_080575.1	100
Fcgrt	Forward: CCTCAAGACCCTGGAGAAGA Reverse: CCGTGGGCACTGAGGAATTA	NM_010189	96
Lst1	Forward: ATCTGCTTGTGCCGGTTCAG Reverse: CTGGCAGCTGCTGGAGAGA	XM_359281.1	100
Emp3	Forward: GCTTTTTGTGGCCACTTTGG Reverse: TGTTTGAGTGGTGGTGTTCCA	NM_010129.1	100
5830436K05Rik	Forward: ACATTCGAAGGAACCTGGCT Reverse: AATCCTGCAGCACAAACAGC	XM_488874	99
Arhgdib	Forward: TTCTCCCACCTTGAGTCCTGAA Reverse: GGAAGAACCCAGTGGCAAGA	NM_007486.1	101
Marcks	Forward: GTCTCCACCCTGCCCATTT Reverse: AACAGTAACCATTCCACGTATCACA	NM_008538.2	102
Bex2	Forward: TGGAGAAGCTGAGGGAAAGG Reverse: CAGGGCATAAGGCAAAACTCAT	XM_977338.1	100
Endod1	Forward: GCTAATGGAAGCCAGTCATGGT Reverse: AGCCTGTCGTCTTGATGGTGAT	NM_028013.2	100
AI428936	Forward: TGGCCACCGGAAACATTTAG Reverse: CAGCATTGCATCAGGCAGACT	NM_153577.2	100
Slc40a1	Forward: GCCTTAAGGGCTAGGAGCAC Reverse: GACTGCCTCTCCCTCTTCCT	NM_011400.2	98
Bok	Forward: GAGAAGCCAGGGATGCAGAGT Reverse: TGGTTCCTGCCATGAAGGA	NM_016778	100
Mest	Forward: CCTCCCCCATTCTCGTATCTG Reverse: GTGAAGGAAATGGACTTTGATGAA	NM_008590.1	100
Anxa5	Forward: GATTTGATGGCAGGGCTGAT Reverse: TTGCTTCGGGATGTCAACAG	NM_009673.1	100
Peg3	Forward: CCCCTTGAGACTGATTGTGTAACC Reverse: TTTGCAAGAAAACCACTGTAAGGTA	NM_008817.2	106
7530408C15Rik	Forward: CGATCCTGGGACAAACACTTG Reverse: TCCAACTACGTACAGTAGCCCATTC	NM_001195075.1	100
Klhl5	Forward: TTTCATGGAAGTAATCAGGAACCA Reverse: CTCCTCGTTCGGGATGTTCA	NM_175174.2	100
Slc2a1	Forward: ACCTCTTCCGAACCGACAGA Reverse: TGGAGCCATCAAAGTCCTGAA	NM_011400.2	100
Dcbld1	Forward: CGGCCATGACTGCTCTTTTG Reverse: ACATGCACGCTTGCACATTT	NM_025705.2	103

Trp53rk	Forward: GGTGTCTTAAGAGGGCACCA Reverse: GCCTTTCCACAGGACCAGAG	NM_023815.4	101
Ddit4	Forward: AGGTTGTATGCAGGTGGCTC Reverse: TACACATCCAGCCAGAAGCC	NM_029083.1	100
Gata2	Forward; CACCCCTATCCCGTGAATCC Reverse: AGGGCTCAGCAGTAGAGAGT	NM_008090.4	100
Cnih4	Forward: GTGCTGATGCTTGTCTCCCT Reverse: GTTGCCACTTGGCACCATAA	NM_030131.2	100
Xist	Forward: AAAACGGGAAGAGGCCAGAG Reverse: GTGTTCTGCATGCTTGGTCC	NR_001463.2	101
Tiam1	Forward: GGAAGGCTACAGCTTCCTGA Reverse: CCACAATGGTTCTACCCGCT	NM_009384.2	100
Grm6	Forward: AGAGTCCTCCCTTGGTGTGT Reverse: CAGAAGCCTCAGTCCAGAGC	NM_173372.1	98
Cap1	Forward: CGCCTCCTCCCCCAATTC Reverse: TGTGTGATGCTTTCCCCCTG	NM_007598.2	97
X99384	Forward: TGAAGAAGGAGGTGGATGCG Reverse: TGCCTGTCGGTAGGTGGATA	NM_013753.1	101

Supplementary Table S2: List of 370 differentially expressed genes by microarray analysis.

The table shows normalized intensities of AGM-derived HSC at 9.5 dpc and 10.5 dpc (n = 3), ratio (non-log fold-change), p-value and adjusted p-value.

Probe ID	Symbol	AGM-derived HSC at 9.5 dpc			AGM-derived HSC at 10.5 dpc			ratio	p-value	Adjusted p-value
		Sample#1	Sample#2	Sample#3	Sample#1	Sample#2	Sample#3			
2970324	*Hdc*	830.25	935.83	231.57	9519.32	9364.16	7794.57	15.69	0.00014	0.07378
4880386	*Muc13*	291.20	293.79	650.28	3445.93	2988.55	2794.07	8.03	0.00005	0.06115
6550500	*Slc41a3*	220.98	223.15	339.68	3891.32	1252.49	669.85	5.80	0.00448	0.12896
5890719	*Fam110b*	365.57	389.56	281.13	3673.80	1807.58	1157.27	5.77	0.00053	0.08413
160327	*1700012H17Rik*	367.81	397.98	317.76	3509.98	1887.92	1267.01	5.65	0.00026	0.08153
2340484	*Unc13d*	274.09	280.67	1171.16	2492.29	3366.98	1897.98	5.61	0.00386	0.12220
5720609	*Lyz*	355.62	371.78	610.36	1701.37	2622.91	2588.35	5.23	0.00007	0.06715
1340092	*Unc13d*	256.82	252.24	755.13	2137.08	2353.34	1211.12	4.99	0.00211	0.10870
5960717	*C230009C22Rik*	369.61	404.06	466.08	3182.19	2818.14	921.41	4.91	0.00179	0.10232
7570228	*Chd2*	269.20	270.92	240.68	455.97	1911.28	2187.25	4.77	0.00606	0.14063
1570594	*Socs3*	1271.77	1272.89	3891.32	13433.56	7015.73	7095.24	4.73	0.00292	0.11416
6940132	*A230050P20Rik*	807.34	875.24	1334.95	8202.50	4610.44	2622.14	4.72	0.00128	0.09534
4880026	*Tspan17*	290.23	311.85	533.15	4201.84	1270.65	887.80	4.61	0.00702	0.14724

4150725	*Ctsz*	840.91	738.73	2187.25	7425.53	4503.58	3403.05	4.38	0.00309	0.11416
150458	*Trp53rk*	458.18	409.77	277.21	1917.66	2082.78	1026.80	4.29	0.00041	0.08299
4540626	*Tmem38b*	790.50	805.67	280.14	3551.82	1980.80	1806.46	4.15	0.00361	0.12045
6450438	*Stk38l*	228.80	225.86	835.59	1305.11	2227.71	1005.70	4.08	0.00920	0.16242
7040446	*Gfi1*	344.45	371.11	622.49	2573.71	1688.22	1178.57	4.01	0.00079	0.08614
450615	*Bbc3*	1096.15	886.40	4279.67	12257.64	6436.76	3363.15	4.00	0.02527	0.22570
6330717	*LOC100044776*	773.77	856.84	1502.20	5399.21	3953.60	2897.70	3.96	0.00060	0.08413
6860253	*H13*	1476.47	1365.00	263.33	3886.80	3006.20	2820.69	3.96	0.01882	0.20295
3450091	*Ctsz*	743.48	674.68	1745.53	5793.72	3914.03	2397.59	3.96	0.00367	0.12071
1110202	*Camkk2*	1579.67	1599.46	1961.20	10155.45	7161.22	4152.41	3.94	0.00057	0.08413
6200719	*Acss1*	410.76	446.32	252.09	1630.10	1529.18	1126.99	3.93	0.00018	0.07378
4540564	*Dok2*	261.14	265.47	342.33	1220.66	1229.69	881.23	3.82	0.00003	0.06115
130634	*Ddit4*	568.31	588.80	1092.67	3363.15	2332.50	2439.05	3.74	0.00042	0.08299
1050092	*Serpina3g*	267.80	262.82	247.66	568.66	1324.19	1180.30	3.71	0.00069	0.08413
6580021	*Mpo*	3535.14	3506.52	3883.81	9975.33	12586.18	17879.26	3.60	0.00010	0.07378
7510390	*4933439C20Rik*	788.54	832.69	550.99	3261.82	2910.35	1664.35	3.52	0.00058	0.08413
270673	*Acads*	1903.60	2058.83	7292.12	15463.33	11386.26	7088.47	3.52	0.01486	0.18482
3520546	*Emp3*	716.26	763.21	1184.15	2313.10	3998.36	2731.26	3.39	0.00048	0.08413

4200204	*Sh3bp2*	711.78	727.29	4035.31	6692.16	4543.87	2679.31	3.39	0.04430	0.26916
4900403	*Gnas*	462.38	502.92	270.39	818.76	2231.59	1330.63	3.38	0.00380	0.12168
2940681	*Gata2*	3451.52	3246.33	4606.56	16151.05	8857.75	13501.76	3.34	0.00035	0.08299
6660634	*Irf1*	2094.55	2194.27	3858.86	11473.01	7184.64	7955.19	3.33	0.00072	0.08413
1470170	*Ccbl1*	359.57	360.48	607.53	2017.24	1393.67	1033.32	3.33	0.00102	0.09198
7160044	*Cyth4*	1958.18	1977.98	6589.56	9936.96	11345.42	8337.98	3.33	0.00871	0.15965
4060593	*Vangl2*	450.57	481.80	579.40	1761.05	1908.88	1337.61	3.29	0.00005	0.06115
6620685	*Lgals8*	516.74	482.07	781.30	2691.01	2203.52	1162.80	3.28	0.00195	0.10631
4390239	*Fcho1*	294.88	295.02	491.64	1180.30	1517.40	831.36	3.27	0.00082	0.08622
7380630	*E330016A19Rik*	745.37	749.89	1608.78	2546.40	3501.82	3451.52	3.25	0.00150	0.09965
2570672	*Atp2a3*	1558.48	1620.16	5155.74	10012.60	6948.49	6383.68	3.24	0.00999	0.16502
2480343	*A430106G13Rik*	295.93	318.74	1230.25	1299.75	1624.65	1849.68	3.23	0.01761	0.19827
3830524	*Magee1*	400.86	420.21	2221.63	2790.58	2117.67	2014.87	3.17	0.03826	0.25410
5270209	*C330013J21Rik*	222.12	222.64	390.58	1006.01	1032.91	591.39	3.17	0.00131	0.09534
3710136	*2310033F14Rik*	1221.39	1252.03	3535.14	9071.22	4757.79	3944.45	3.16	0.01296	0.17741
6900465	*Plcb2*	629.39	630.28	1063.78	3410.85	2131.37	1817.44	3.15	0.00125	0.09486
2450113	*Stab2*	421.05	434.95	323.07	2382.44	1109.34	641.20	3.06	0.00979	0.16491
2340349	*Aldh2*	6097.19	5775.55	12288.13	28741.38	22247.96	19029.61	3.04	0.00190	0.10618

1450333	*Clec7a*	246.66	231.57	251.49	753.09	821.82	648.83	3.03	0.00002	0.06115
130370	*LOC677144*	394.51	422.19	1013.27	2721.83	1358.65	1255.98	3.02	0.01020	0.16502
7400397	*D530007E13Rik*	328.70	334.42	493.41	1864.39	925.16	862.91	3.02	0.00228	0.11264
940541	*Fcrls*	423.85	433.03	326.64	1168.86	1097.15	1270.86	3.01	0.00004	0.06115
1230040	*5730525O22Rik*	890.26	1037.22	2213.81	6006.11	3727.42	2353.34	2.95	0.01115	0.17066
6590167	*Fcgrt*	405.36	404.52	274.40	1159.82	1011.28	975.14	2.94	0.00013	0.07378
4850594	*Hmha1*	2110.48	2313.75	4046.22	9601.63	8702.41	5933.97	2.93	0.00160	0.10081
2350017	*Hspa1a*	493.41	475.21	231.57	1214.61	822.78	1340.56	2.91	0.00309	0.11416
6560703	*H6pd*	716.00	699.21	2592.43	3310.16	3322.62	2883.86	2.90	0.01873	0.20279
3310400	*Gp5*	230.57	235.28	809.52	910.10	1138.43	1014.42	2.88	0.01673	0.19343
4390022	*Lrrc28*	347.19	351.32	621.78	1485.51	1318.57	925.32	2.88	0.00140	0.09834
6520075	*Ier3*	4913.47	5294.77	8125.00	23512.67	17426.03	12104.34	2.86	0.00170	0.10205
6180411	*Gltp*	449.79	447.08	1411.06	2998.87	1915.51	1137.06	2.84	0.02802	0.23120
2810685	*Glipr1*	416.41	393.17	377.65	842.75	1621.14	1034.60	2.84	0.00061	0.08413
5270608	*Vav1*	1510.09	1639.32	2461.14	4689.37	6471.30	4577.63	2.84	0.00052	0.08413
5270279	*Alox5ap*	958.02	900.19	2103.18	2773.87	4134.68	3553.41	2.82	0.00415	0.12608
7320181	*Slc39a11*	282.78	273.46	615.90	1484.09	973.76	727.23	2.80	0.00742	0.15057
1990437	*Stac3*	266.61	257.08	244.40	1094.18	776.19	429.61	2.79	0.00306	0.11416

60673	*Pip4k2c*	380.48	390.15	1061.17	1529.18	1467.00	1523.20	2.79	0.00777	0.15359
940309	*Mpo*	11146.78	10513.86	11450.52	31002.28	29213.21	31831.42	2.78	0.00001	0.06115
1010196	*Zfp341*	303.61	315.71	246.30	806.63	856.22	719.41	2.76	0.00005	0.06115
5360300	*Lpl*	2143.21	2229.51	5024.87	10126.49	7221.37	6887.72	2.76	0.00509	0.13498
5960347	*Als2*	1007.66	944.77	2432.73	3522.29	3504.36	3879.86	2.74	0.00551	0.13683
5890110	*Cbfa2t3h*	485.30	469.23	402.02	880.60	1267.90	1667.39	2.73	0.00074	0.08538
3420500	*Oxct1*	351.58	378.14	268.58	914.24	721.10	1094.46	2.72	0.00033	0.08299
5860154	*Lst1*	643.90	674.92	767.84	1547.38	2280.48	1888.36	2.71	0.00013	0.07378
2140221	*Slc40a1*	306.05	313.44	303.61	756.40	692.31	1107.46	2.71	0.00023	0.07845
10730	*Cbx6*	665.35	708.29	1834.10	1605.21	4596.28	2323.10	2.71	0.02803	0.23120
4010019	*Ifitm1*	356.81	359.28	544.95	898.00	1241.18	1242.20	2.71	0.00053	0.08413
4890041	*Ilvbl*	2209.98	2353.92	3690.98	7054.43	8942.33	6003.37	2.70	0.00088	0.08899
3800482	*2310047C04Rik*	617.41	574.54	1118.16	3343.13	1736.66	1333.22	2.69	0.01002	0.16502
4920600	*C230071H18Rik*	310.77	317.44	227.28	827.79	700.74	745.87	2.68	0.00012	0.07378
7040307	*2810410C14Rik*	392.77	434.72	274.21	667.64	2151.06	621.87	2.67	0.02403	0.22170
3450180	*Tmem176b*	484.93	401.78	1307.22	1795.99	1819.34	1480.76	2.67	0.01421	0.18086
1030682	*Slc11a2*	312.71	310.94	229.85	980.74	638.37	677.16	2.67	0.00047	0.08413
3420139	*Il1r2*	218.76	219.05	543.73	732.41	813.37	828.45	2.67	0.00626	0.14207

2070243	*Aldh5a1*	784.40	745.37	1760.07	3104.34	2740.18	2290.93	2.67	0.00513	0.13498
4180647	*Zkscan6*	1499.96	1566.12	406.21	2921.90	2817.22	2180.62	2.66	0.03059	0.23812
2900327	*Pfkfb4*	417.64	478.62	1338.32	1775.55	2484.23	1139.38	2.66	0.02573	0.22570
2470424	*2310004H21Rik*	602.50	665.60	1098.70	3264.73	1448.19	1745.21	2.66	0.00661	0.14406
1500301	*Tuba8*	508.29	484.93	825.61	2550.60	1381.43	1065.07	2.64	0.00693	0.14652
3400646	*Sirpa*	2027.71	2149.26	3108.64	6924.06	6811.32	5250.19	2.63	0.00042	0.08299
6940040	*Msi2h*	884.37	1016.97	804.00	2794.07	2475.38	1872.08	2.62	0.00024	0.07845
7610356	*Dynll2*	213.00	213.86	238.84	1308.94	263.93	560.47	2.61	0.03605	0.25022
6420520	*Fosb*	525.66	547.15	1099.79	3474.18	1259.02	1275.56	2.60	0.02382	0.22105
6270091	*Stk17b*	265.19	270.00	553.00	888.50	822.78	931.45	2.58	0.00282	0.11416
1410113	*Uap1l1*	617.69	558.35	1404.71	2271.66	2471.12	1458.30	2.57	0.01110	0.17066
5910681	*Als2*	890.52	860.13	2311.52	2960.76	3019.18	3298.44	2.55	0.01013	0.16502
7200189	*C330006A16Rik*	1342.35	1374.58	3296.26	4966.77	6097.19	3311.78	2.55	0.01315	0.17818
5340762	*AW212394*	332.27	332.81	325.22	1139.38	687.94	751.36	2.54	0.00047	0.08413
540437	*Nfatc2ip*	320.78	318.92	491.26	1201.84	1021.97	641.49	2.50	0.00288	0.11416
1030053	*Mta2*	4157.22	3896.60	10829.65	16542.26	13678.29	12139.00	2.50	0.01377	0.17917
4850291	*Pik3cg*	260.95	268.90	448.50	1308.04	687.16	545.99	2.50	0.00986	0.16502
3710215	*Map2k7*	444.15	457.98	701.29	2182.83	1308.04	773.66	2.49	0.01263	0.17711

6290768	*Cd52*	586.94	586.94	936.07	755.79	2793.40	2336.51	2.48	0.03595	0.25022
5090445	*Unc84b*	1199.88	1121.46	2209.98	3425.66	4137.66	3163.46	2.47	0.00276	0.11406
6330543	*Glrx1*	578.72	582.47	436.87	1298.59	1106.34	1542.85	2.47	0.00033	0.08299
1770201	*Serinc3*	2286.66	2675.05	2687.78	8915.72	5165.93	5311.72	2.46	0.00114	0.09418
2750594	*Tmem51*	553.95	569.17	400.25	1428.33	1817.44	720.98	2.46	0.00868	0.15965
7000300	*2900006A08Rik*	334.92	319.99	516.49	1167.80	1091.51	643.81	2.46	0.00357	0.12013
270228	*Stard5*	330.04	330.04	459.85	1159.60	1029.96	620.98	2.46	0.00243	0.11313
4050112	*Glrx*	533.15	527.00	303.30	1039.52	813.93	1462.01	2.44	0.00439	0.12808
5560470	*Psap*	2675.05	2931.87	6700.35	10964.97	8759.81	7937.85	2.44	0.01007	0.16502
1230612	*Aqp1*	465.05	478.29	726.76	1470.72	1495.44	1058.21	2.43	0.00117	0.09418
4180458	*Etfa*	980.22	1097.15	1627.98	4270.28	2124.81	2765.13	2.43	0.00474	0.13086
5290170	*Zfp180*	737.26	821.97	2332.50	3953.60	2540.88	2013.08	2.43	0.03328	0.24207
2140753	*Grina*	930.84	962.16	1122.32	1904.34	3324.55	2265.21	2.43	0.00098	0.09054
5960341	*Msrb2*	525.39	466.33	582.00	1973.25	1106.62	928.62	2.42	0.00349	0.11952
6250291	*Rpia*	416.98	425.81	440.02	1477.21	893.91	838.26	2.42	0.00112	0.09418
3310091	*LOC100048589*	1255.62	1213.55	1111.72	2796.02	3017.69	2839.62	2.42	0.00004	0.06115
4480093	*LOC225897*	1999.61	2010.75	2663.46	6107.17	6011.72	4125.31	2.42	0.00070	0.08413
6580711	*LOC100044172*	817.17	857.21	2498.83	2219.09	3572.96	3108.64	2.41	0.02707	0.22755

3170577	*Pla2g15*	2871.81	2796.34	7473.80	10608.51	10829.65	7239.23	2.40	0.01803	0.19933
6650477	*Gimap6*	1630.89	1835.12	4274.85	6075.00	6940.70	4112.37	2.38	0.01725	0.19544
3420689	*EG665369*	564.30	513.53	1065.72	1541.44	1648.03	1647.11	2.38	0.00344	0.11945
7330026	*Egr2*	358.03	355.36	300.41	932.05	492.95	1120.51	2.38	0.00535	0.13600
5340270	*Epc1*	811.98	851.12	1310.72	4656.54	2257.81	1155.51	2.38	0.04062	0.25987
2060373	*Cd79b*	672.24	636.28	367.02	2151.57	1103.85	883.40	2.37	0.01541	0.18801
6900632	*1810026J23Rik*	732.41	806.84	1948.78	3087.67	2487.88	1987.68	2.37	0.01682	0.19343
2940504	*Ncf4*	225.85	238.01	348.42	473.75	623.45	836.70	2.36	0.00265	0.11406
3360138	*Irf1*	494.58	486.81	720.98	1408.29	1141.69	1423.08	2.36	0.00060	0.08413
6290193	*2510010K19Rik*	519.27	515.93	929.13	1651.44	1800.59	1102.20	2.36	0.00486	0.13213
6280168	*Mpo*	526.28	528.24	452.79	1190.50	1189.41	1168.86	2.36	0.00005	0.06115
7330110	*Crtc3*	485.30	458.29	474.27	1982.96	945.96	739.13	2.36	0.01044	0.16624
2900139	*Ube2e2*	538.54	502.92	257.20	1324.48	961.74	718.02	2.36	0.01013	0.16502
7000497	*Ssr1*	876.59	956.77	1315.87	2579.23	2729.11	2055.49	2.36	0.00067	0.08413
3120563	*Fbf1*	560.03	543.83	394.18	2212.62	1085.54	654.93	2.36	0.02476	0.22472
3800603	*Slc22a3*	259.33	238.26	371.88	1017.91	651.15	452.17	2.35	0.00734	0.14998
7100392	*Pop1*	254.59	251.38	332.80	825.25	640.46	525.00	2.35	0.00084	0.08736
110717	*AI428936*	333.19	363.03	302.05	815.43	884.37	656.69	2.35	0.00020	0.07472

2900255	*Wsb2*	539.95	549.16	977.28	2112.29	1566.71	1132.64	2.35	0.00679	0.14539
2370390	*Krtcap3*	652.96	694.71	381.31	1261.53	1609.28	1100.95	2.35	0.00315	0.11550
4390148	*Rhox5*	401.80	398.74	389.03	1198.64	1038.47	630.86	2.33	0.00199	0.10681
3800630	*Fbxl20*	523.12	533.15	673.60	2364.42	1070.59	929.80	2.32	0.01210	0.17462
1070224	*Emp3*	255.03	263.50	224.43	495.00	657.36	572.78	2.31	0.00018	0.07378
3140279	*A130052D22*	230.50	229.90	687.66	801.98	964.60	581.93	2.31	0.03362	0.24290
10402	*Trim25*	2509.13	2037.49	3553.41	11295.76	3715.45	5306.50	2.31	0.02620	0.22613
3800601	*Muted*	3448.87	3556.62	2173.05	5736.32	8954.25	6293.42	2.30	0.00290	0.11416
150209	*A430006M23Rik*	321.02	334.22	311.77	662.19	994.99	614.57	2.30	0.00081	0.08614
1710754	*Ctsc*	648.38	635.17	470.52	1383.33	1101.09	1535.67	2.29	0.00066	0.08413
1940608	*Lyzs*	224.43	218.38	255.46	442.36	649.82	522.49	2.29	0.00039	0.08299
1070152	*Stxbp2*	3969.90	3775.46	4718.20	7837.02	10414.45	10372.06	2.29	0.00034	0.08299
2370437	*BC031781*	1583.49	1775.75	1041.55	5867.11	3089.98	1925.44	2.28	0.02621	0.22613
4040563	*4631409F12Rik*	1031.10	1094.97	1256.64	3998.36	2351.74	1791.89	2.28	0.00557	0.13683
2030382	*A930023F12Rik*	255.98	272.18	277.70	662.82	492.38	700.44	2.28	0.00032	0.08299
6250600	*Cdkn2d*	468.58	454.39	1241.35	2397.59	1408.29	923.51	2.28	0.04857	0.27915
6130014	*Iqgap2*	1964.18	2137.08	1228.52	6576.75	2894.81	3171.53	2.27	0.01550	0.18837
5050437	*Ccrk*	403.76	440.73	762.90	1275.82	1693.28	730.85	2.27	0.01678	0.19343

2030368	*9130404D08Rik*	761.20	739.13	1178.57	2034.09	2229.51	1691.25	2.26	0.00145	0.09920
3840273	*Zzz3*	545.01	607.49	794.02	1486.79	1505.84	1338.32	2.25	0.00040	0.08299
2570451	*Mrps23*	969.60	902.77	1710.25	3193.38	2422.83	2203.52	2.25	0.00492	0.13223
2570187	*Zfp87*	354.62	346.95	619.92	1329.30	1062.04	614.38	2.25	0.01369	0.17917
290632	*Axin1*	5243.75	5162.52	16829.94	17686.21	19844.03	14711.51	2.25	0.04079	0.26008
6940324	*Rassf4*	224.20	235.83	249.88	554.77	629.07	426.88	2.24	0.00042	0.08299
7330292	*Mgst2*	289.81	290.25	958.42	1009.15	1156.28	772.66	2.24	0.04687	0.27624
450368	*Rgs1*	330.54	349.25	387.80	1151.15	623.59	696.72	2.24	0.00257	0.11406
5080450	*4833426J09Rik*	1519.20	1650.08	641.78	2574.71	2583.13	2699.70	2.23	0.01504	0.18618
5260433	*Agtrap*	391.11	379.20	635.72	1331.33	1092.60	722.28	2.23	0.00666	0.14406
10717	*B9d2*	1079.77	1069.03	2220.78	3180.46	4152.41	2154.29	2.23	0.01632	0.19263
70414	*5730601F06Rik*	2162.39	2320.43	6174.38	9376.47	7705.11	4721.98	2.22	0.04061	0.25987
2230477	*Mmp24*	344.23	365.22	1027.97	1161.85	1441.35	844.86	2.22	0.03836	0.25410
6620735	*2310036D04Rik*	464.28	452.47	1052.73	1631.83	1394.44	1061.74	2.22	0.01604	0.19159
4900678	*9030619K07Rik*	2079.13	2224.37	3971.28	7497.79	6393.31	4178.46	2.22	0.01003	0.16502
7330131	*A630006E02Rik*	453.13	426.73	327.98	665.87	1143.01	903.00	2.21	0.00227	0.11264
4220008	*Tmem81*	380.01	377.59	290.71	750.84	882.41	678.36	2.21	0.00045	0.08413
5290402	*4933407N01Rik*	365.34	383.16	364.38	1394.90	520.84	750.38	2.20	0.01351	0.17914

7000438	*Bat2d*	698.57	693.08	989.35	3331.39	1472.63	1038.94	2.20	0.03252	0.23995
6270131	*Pqlc1*	764.18	710.97	346.90	1239.73	1011.97	1593.29	2.20	0.01302	0.17785
6900470	*Mrpl16*	787.03	711.37	719.52	2005.61	1428.52	1489.51	2.20	0.00041	0.08299
450561	*Frmd4a*	293.48	302.09	238.01	969.90	579.11	396.14	2.19	0.01081	0.16852
4010670	*2700033B16Rik*	433.20	439.89	487.68	1472.63	769.78	860.54	2.19	0.00355	0.12013
6290379	*Sdad1*	1385.78	1395.21	3564.67	5539.06	4102.78	3183.19	2.19	0.02946	0.23433
3360048	*Keap1*	522.76	552.38	838.83	1656.06	1243.17	1231.73	2.19	0.00211	0.10870
4010133	*Cdc42ep4*	1189.00	1163.37	1920.25	4786.91	2981.88	1944.65	2.19	0.01803	0.19933
630091	*Nfkbid*	621.39	617.69	985.41	1527.41	1767.68	1461.32	2.18	0.00159	0.10081
2190066	*Tmem38b*	398.57	390.95	253.61	833.89	676.75	730.13	2.18	0.00141	0.09834
2100497	*LOC621823*	375.65	351.42	552.62	1206.05	830.08	755.94	2.18	0.00343	0.11945
1170170	*Nfe2*	934.40	996.34	599.20	1545.17	1764.74	2081.65	2.17	0.00243	0.11313
6660039	*Mad*	444.90	423.65	932.46	955.01	1470.72	1268.89	2.16	0.01432	0.18175
1010601	*Napa*	565.37	522.09	535.24	2496.16	981.63	652.20	2.16	0.04718	0.27730
6110577	*1110003E01Rik*	623.63	592.94	830.25	1890.20	1287.91	1274.51	2.16	0.00178	0.10205
1510669	*Acy1*	842.34	864.27	1407.39	2435.44	2244.97	1863.28	2.15	0.00274	0.11406
4010097	*Map4k1*	558.74	557.57	1463.58	1247.08	2367.69	1523.49	2.14	0.03965	0.25599
3460762	*Rasgrp4*	794.74	823.88	1560.62	2335.16	2814.25	1510.09	2.13	0.01587	0.19083

4060240	*Ptpn6*	1902.08	1958.18	2009.63	3233.71	4683.26	4774.31	2.13	0.00078	0.08614
6760546	*Rbbp5*	326.49	335.92	367.75	574.97	933.42	725.73	2.13	0.00118	0.09418
460692	*Bcl11a*	482.70	412.10	471.60	870.51	860.54	1206.05	2.13	0.00066	0.08413
3390452	*E330019I03Rik*	223.78	226.06	549.58	947.67	574.54	488.41	2.12	0.03647	0.25153
6510041	*Frmd4a*	291.13	301.54	241.90	904.02	573.43	390.00	2.12	0.01018	0.16502
130661	*5830436K05RIK*	241.20	253.50	239.45	461.90	569.42	529.51	2.12	0.00016	0.07378
5310360	*Stat3*	4818.48	4436.46	4963.18	14145.48	8796.27	8015.52	2.11	0.00277	0.11406
1090180	*Arhgdib*	1187.16	1255.51	1424.35	2509.13	2708.39	2936.27	2.11	0.00019	0.07378
5420142	*Churc1*	312.50	317.16	244.04	1065.07	422.33	501.95	2.11	0.01943	0.20497
3140465	*6330548G22Rik*	1139.38	1088.41	1137.06	3572.96	2265.21	1624.11	2.10	0.00730	0.14946
3420528	*4933407N01Rik*	394.78	406.21	330.93	1280.35	540.84	711.54	2.10	0.01239	0.17647
3460392	*Mpl*	799.35	732.41	1197.47	1718.14	1975.22	1915.51	2.10	0.00176	0.10205
4220193	*Pgpep1*	405.04	423.49	787.68	811.50	1230.72	1247.53	2.10	0.01163	0.17309
6620180	*Fnbp1*	11512.36	13207.85	18821.72	46164.40	26090.96	21892.28	2.10	0.01380	0.17917
6860609	*Rbp1*	1552.25	1681.57	1516.40	4582.08	3339.36	2370.40	2.09	0.00390	0.12246
2120014	*Pole3*	1816.07	1945.69	3632.38	7926.70	5186.75	2846.08	2.09	0.04381	0.26863
5670634	*Synpo*	785.59	827.23	1015.40	2238.61	1750.98	1533.53	2.09	0.00110	0.09418
3170672	*Sergef*	284.67	283.27	377.65	613.78	819.10	548.90	2.08	0.00167	0.10205

2690253	*Angptl6*	252.65	255.96	447.83	751.36	953.74	365.37	2.08	0.03508	0.24736
1400523	*Smap2*	2563.26	2393.66	4869.62	4700.35	7278.26	7883.73	2.08	0.01623	0.19247
4540278	*Pcbd2*	787.38	786.38	1208.07	1898.39	2222.16	1585.96	2.08	0.00273	0.11406
4640168	*3110001D03Rik*	2150.54	2063.27	4543.87	7509.61	4869.62	4915.77	2.07	0.02047	0.20904
50079	*Hist1h1c*	535.41	527.80	1087.47	1730.90	1052.61	1492.93	2.07	0.01756	0.19814
4760041	*Tmem160*	1750.16	1792.71	2870.46	6262.75	3847.39	3304.20	2.07	0.01166	0.17309
4280056	*Trib3*	380.19	349.69	511.53	622.90	1058.76	907.72	2.06	0.00449	0.12896
2810315	*Chst3*	280.76	286.10	238.53	650.80	568.95	454.97	2.06	0.00080	0.08614
450088	*9830134C10Rik*	381.41	391.36	362.47	674.34	871.48	806.63	2.06	0.00029	0.08299
3120619	*Myom1*	370.44	350.67	286.59	1369.24	452.44	521.93	2.06	0.04198	0.26309
6650458	*Nfkbiz*	741.01	791.55	517.58	1354.84	1145.18	1698.94	2.06	0.00304	0.11416
4490239	*Znfx1*	614.17	623.59	1490.88	2108.10	1413.95	1662.30	2.05	0.02773	0.23041
6100523	*Cugbp2*	1588.43	1498.82	1212.23	3899.94	2490.17	2561.15	2.05	0.00261	0.11406
360270	*Ppm1b*	5365.70	4601.54	8058.71	18365.09	12288.13	7595.70	2.05	0.02505	0.22570
360524	*2700087H15Rik*	1563.58	1674.44	2804.24	2639.88	6135.43	3874.86	2.04	0.02558	0.22570
1980619	*Ppm1b*	5033.81	4555.59	7946.54	18470.99	11625.30	7230.98	2.04	0.03032	0.23744
3990228	*Tmem44*	541.10	553.95	628.74	1429.02	1195.36	934.33	2.04	0.00121	0.09486
3310538	*Pcbd2*	1151.41	1300.96	2025.15	3221.51	2979.68	2669.10	2.04	0.00364	0.12051

4200224	*Helb*	767.16	753.46	1335.46	2332.50	1754.02	1588.09	2.03	0.00788	0.15486
1110095	*Muted*	6309.46	5634.74	3590.70	8954.25	12621.22	9499.90	2.03	0.00569	0.13749
2030259	*Depdc5*	351.47	337.10	445.24	977.17	739.86	607.45	2.03	0.00262	0.11406
6220044	*Dennd1c*	219.79	216.71	310.10	390.49	563.84	558.00	2.03	0.00295	0.11416
7100291	*Hoxa5*	700.10	660.61	1619.41	1570.18	1500.60	2639.88	2.03	0.03943	0.25555
20064	*Capg*	666.29	656.60	686.11	1591.92	1265.39	1236.88	2.02	0.00036	0.08299
4780184	*Ly6e*	596.81	648.01	676.75	874.38	1309.81	1895.00	2.02	0.00902	0.16162
150035	*Fut8*	812.70	844.72	775.73	1455.46	1551.18	1955.62	2.02	0.00048	0.08413
6980187	*Gria3*	548.71	490.57	400.66	862.91	1004.58	1031.10	2.02	0.00069	0.08413
4610300	*Pet112l*	289.90	291.04	224.43	584.72	592.97	450.12	2.02	0.00108	0.09406
5220279	*Mt1*	4089.44	4209.24	4498.59	6225.31	10372.06	9872.41	2.02	0.00282	0.11416
2070246	*4733401I05Rik*	311.13	321.14	810.19	768.82	1033.32	836.98	2.02	0.03435	0.24477
1690497	*2310043N10Rik*	525.10	535.51	568.55	1524.46	1051.82	813.55	2.01	0.00428	0.12775
160086	*Vamp1*	212.61	212.93	230.72	545.01	256.21	606.54	2.01	0.01882	0.20295
4050437	*Chst3*	285.24	308.38	227.63	624.43	557.40	465.99	2.01	0.00114	0.09418
3610162	*Dbr1*	739.34	712.45	724.53	1842.34	993.06	1686.85	2.01	0.00527	0.13540
6660707	*Klhl5*	529.25	557.07	523.35	332.03	242.45	239.44	0.50	0.00079	0.08614
2370446	*Eif5a*	596.22	741.33	732.09	259.62	405.50	383.80	0.50	0.00254	0.11406

2940164	*Rbm13*	3126.30	2817.68	1389.28	930.44	1047.92	1552.25	0.50	0.02601	0.22586
5270687	*E330020G21Rik*	4714.91	4894.25	1980.80	1688.22	1494.47	2238.61	0.50	0.03274	0.24080
4060609	*9830005G06Rik*	698.66	717.64	471.16	372.70	254.06	304.64	0.50	0.00357	0.12013
4290458	*F730003H07Rik*	867.52	835.59	653.84	336.11	451.80	380.71	0.50	0.00107	0.09406
2750682	*Chd1*	1919.57	2191.34	1651.65	468.10	1455.46	1239.73	0.50	0.04902	0.28042
6590286	*P2ry5*	10101.38	11160.89	7074.16	3390.57	5102.58	5532.61	0.49	0.00616	0.14188
6840433	*Npm1*	25925.63	24957.99	11716.57	13347.47	5964.96	11427.53	0.49	0.04539	0.27169
430576	*Ptprm*	866.52	873.94	469.78	394.47	315.97	341.58	0.49	0.00736	0.15029
3170397	*LOC100045967*	3400.51	3299.86	1681.57	1055.81	1231.26	1733.67	0.49	0.01767	0.19848
3710242	*Arpc3*	3039.31	2871.81	1301.73	774.60	1051.05	1661.58	0.49	0.04273	0.26457
6860333	*A130099L09Rik*	741.52	721.36	691.23	451.15	300.71	322.88	0.49	0.00108	0.09406
4490168	*Wdr74*	3163.46	3120.79	2559.53	942.27	1370.43	2315.24	0.49	0.01662	0.19343
2030091	*Rbm9*	595.00	549.44	401.04	248.41	244.00	254.74	0.49	0.00092	0.09018
5270452	*Tiam1*	3596.56	3369.53	2392.86	1724.77	1283.19	1530.37	0.49	0.00194	0.10631
6510553	*Gnb1*	1177.33	1323.70	749.53	364.54	504.10	741.66	0.49	0.01598	0.19115
7380364	*Carhsp1*	1825.10	1726.53	1120.32	845.42	601.51	808.79	0.49	0.00409	0.12546
1500768	*Dcbld1*	881.68	921.93	710.39	342.22	462.24	422.83	0.49	0.00086	0.08804
2750221	*Bat2d*	960.96	914.15	550.45	434.28	464.04	276.76	0.49	0.01036	0.16598

1820224	*Marcks*	1643.34	1516.90	1400.90	690.10	769.78	743.61	0.48	0.00016	0.07378
6840482	*6330581N18Rik*	1759.07	1866.67	1492.46	1102.65	652.11	770.65	0.48	0.00257	0.11406
670026	*LOC100046650*	2297.80	1977.33	1323.49	708.06	792.97	1207.60	0.48	0.00844	0.15815
1990021	*ENSMUSG00000068790*	2670.29	2471.12	1368.56	1498.25	717.76	946.62	0.48	0.02261	0.21581
1850408	*D130078K04Rik*	1084.35	964.25	665.60	400.18	535.18	365.51	0.48	0.00370	0.12071
3130603	*A630042L21Rik*	905.55	972.20	726.43	435.50	328.63	502.52	0.48	0.00175	0.10205
2470195	*Pcbp1*	1836.19	1624.65	868.06	445.32	618.43	1054.37	0.48	0.03496	0.24732
3290164	*LOC622994*	2177.70	1925.44	1423.70	460.11	1029.03	1408.16	0.48	0.03984	0.25680
5290189	*Dync1h1*	1146.89	1100.52	844.16	306.81	566.90	682.28	0.48	0.01284	0.17711
2490255	*Narg1*	2952.95	2965.26	2159.93	869.84	1253.51	1921.50	0.48	0.01128	0.17166
1990564	*Txndc5*	2098.55	2041.04	2308.43	728.35	1298.59	1153.44	0.48	0.00309	0.11416
4040768	*Rn18s*	1901.37	1817.99	996.77	485.30	800.34	974.78	0.48	0.01978	0.20633
2810634	*Sept11*	17879.26	21606.02	8833.80	7109.72	6844.10	7659.39	0.48	0.01508	0.18634
1260164	*Asns*	2890.38	2628.47	1455.46	879.10	1145.47	1189.00	0.48	0.00819	0.15762
6760538	*Prkd3*	2489.73	2256.11	1170.52	1058.21	786.83	853.91	0.48	0.01087	0.16911
2100221	*LOC270589*	886.96	821.49	438.88	428.48			0.47	0.01212	0.17462
2710544	*Gli3*	2158.49	2176.83	2145.13	1442.50	787.68	918.77	0.47	0.00274	0.11406
7200240	*Sap30*	3082.42	3142.32	2155.21	946.15	1409.03	1614.79	0.47	0.00409	0.12546

1240564	*Appbp2*	10372.06	10952.90	5566.06	2765.13	4440.31	5274.55	0.47	0.01657	0.19343
3140370	*Nid1*	1750.74	1931.27	804.44	791.97	728.73	480.40	0.47	0.02274	0.21601
2510037	*Alad*	4342.34	4863.18	3233.71	1310.29	2177.70	2429.57	0.47	0.00613	0.14188
3370487	*Ext1*	1651.44	1828.19	1439.70	415.02	1049.43	1011.63	0.47	0.02095	0.20988
5890255	*Cd93*	2063.27	2121.89	798.74	642.94	587.08	937.03	0.47	0.03230	0.23952
7330551	*Sall4*	835.39	826.20	335.28	291.95	270.71	291.60	0.46	0.01851	0.20217
4880554	*Cnih4*	2341.05	2386.38	1591.44	872.82	975.52	1036.81	0.46	0.00098	0.09054
6980025	*Shroom2*	3105.63	3111.46	1964.18	1122.03	1059.21	1551.18	0.46	0.00304	0.11416
6940068	*X99384*	1487.66	1339.79	1286.74	755.13	501.51	657.07	0.46	0.00066	0.08413
6900017	*Bzw1*	2699.70	2341.05	1549.32	581.05	827.39	1968.44	0.46	0.04597	0.27279
2710328	*C230070D10Rik*	2452.64	2636.25	1318.94	871.72	1051.39	898.07	0.46	0.00566	0.13725
5080114	*D130047L08Rik*	615.22	678.06	647.06	247.10	337.12	312.28	0.46	0.00030	0.08299
450372	*Bok*	2243.17	1962.47	2329.19	842.41	945.04	1235.39	0.46	0.00060	0.08413
2490113	*Lin28*	582.94	507.24	1264.77	284.55	375.37	333.39	0.46	0.01537	0.18801
1580088	*Ccnd2*	3136.60	3274.47	1117.18	1268.72	792.66	1078.32	0.46	0.03699	0.25198
	Mogat2	698.27	716.26	772.59	307.48	344.58	344.01	0.46	0.00008	0.07262
1030338	*Atp5c1*	6368.01	6622.65	3180.46	2130.52	1990.15	2951.52	0.45	0.01007	0.16502
1980392	*Galnt1*	877.53	864.66	430.84	292.53	297.91	344.65	0.45	0.00638	0.14319

6130561	*Plau*	591.95	607.16	1015.68	290.16	318.30	362.12	0.45	0.00233	0.11289
5860494	*5830406C17Rik*	720.72	714.55	744.67	308.67	309.08	365.72	0.45	0.00009	0.07378
6520040	*Heatr5a*	873.21	861.10	382.87	308.69	338.81	248.31	0.45	0.01256	0.17711
3190408	*Mest*	2336.51	2268.08	2692.25	814.69	1242.20	1239.92	0.44	0.00091	0.09005
610253	*Eno1*	5634.74	5800.43	2535.02	1620.16	1583.49	2825.66	0.44	0.02029	0.20777
7160725	*C230029D21Rik*	1927.75	2031.28	1732.36	916.31	746.70	842.07	0.44	0.00012	0.07378
990435	*Dynll1*	10291.20	9023.06	3868.21	3603.73	2511.25	3356.93	0.44	0.01810	0.19965
2060008	*Rsrc2*	728.78	808.42	297.75	232.77	248.64	250.78	0.44	0.01585	0.19081
5810168	*Nfatc3*	1130.35	1175.78	641.45	381.38	408.68	445.95	0.43	0.00240	0.11289
2710324	*Aard*	1019.03	979.84	1569.55	806.37	477.39	320.54	0.43	0.01264	0.17711
130594	*D930048N14Rik*	3955.69	4780.48	3328.80	1258.10	2641.40	1476.47	0.43	0.00525	0.13540
1690091	*Vim*	1234.81	1340.99	691.55	373.42	422.82	564.10	0.43	0.00465	0.13037
6760008	*Ypel5*	911.49	971.94	324.82	296.64	240.04	313.88	0.43	0.02391	0.22145
630600	*Eif3eip*	2897.70	2305.12	1008.12	681.32	712.86	1075.67	0.43	0.02099	0.20988
3440343	*Cap1*	952.25	998.10	550.70	310.26	330.02	393.64	0.43	0.00225	0.11264
70400	*2610104A14Rik*	976.16	981.84	429.50	285.06			0.43	0.00944	0.16333
730739	*Cep78*	1612.75	1676.36	583.48	448.11	447.96	603.35	0.43	0.02232	0.21524
6350044	*Slc2a1*	7385.06	7320.20	4586.46	2559.53	2795.69	2645.31	0.42	0.00083	0.08659

2030692	*D130071N09*	4811.10	5812.17	4894.25	1238.97	2857.82	2894.81	0.42	0.00885	0.16088
6060376	*Orc6l*	1851.62	1697.73	735.92	604.11	426.77	659.04	0.42	0.01369	0.17917
3290747	*Bex2*	3216.97	3492.91	2793.40	1537.72	1210.87	1237.43	0.42	0.00016	0.07378
5290148	*Setd5*	1205.49	1197.63	449.89	258.50	347.01	527.75	0.42	0.02715	0.22765
2350079	*A730094H17Rik*	2487.20	2977.58	857.76	866.90	685.15	774.89	0.42	0.02866	0.23278
3990484	*3110004L20Rik*	1740.60	1768.32	1503.83	638.90	752.33	686.64	0.41	0.00007	0.06715
1980487	*4921506J03Rik*	5465.30	6097.19	2894.81	1420.41	2074.70	2294.71	0.41	0.00649	0.14345
3840300	*E130012P04Rik*	614.48	619.99	597.68	230.44	222.10	311.03	0.41	0.00018	0.07378
780093	*Cox6b1*	2419.34	2278.11	706.23	421.00	672.78	956.54	0.41	0.04830	0.27829
1740553	*Raf1*	3480.68	3104.34	1595.08	879.32	1028.61	1323.09	0.41	0.00604	0.14049
3990500	*5330408N05Rik*	1674.44	1744.52	921.03	383.95	799.68	586.01	0.41	0.00823	0.15777
6940136	*Mllt4*	5682.19	6214.35	1527.41	1671.72	1208.77	1772.05	0.40	0.04637	0.27410
1710504	*Isg20l2*	1376.83	1388.78	947.04	314.70	445.99	833.89	0.40	0.00957	0.16367
4040037	*Tpm4*	16123.05	16050.96	9418.58	4319.04	4361.23	8234.12	0.40	0.00578	0.13838
7610494	*Ssr2*	2892.86	3080.86	1975.85	654.93	1048.58	1614.26	0.40	0.00728	0.14946
	7530408C15Rik	4395.28	4543.87	5979.14	2324.44	2188.63	1465.30	0.40	0.00077	0.08610
6510333	*Sfrs1*	10437.95	10069.31	3574.95	2311.52	1757.86	5593.79	0.39	0.04944	0.28050
2570196	*Soat1*	1208.34	1418.84	341.34	292.44	301.24	400.31	0.39	0.03873	0.25410

6770356	*Mest*	7257.15	6954.87	7505.60	2006.52	2951.52	3837.83	0.39	0.00100	0.09078
2000180	*Prdx4*	4698.57	4015.76	1915.51	884.61	1280.11	1913.65	0.39	0.01441	0.18232
6290133	*Endod1*	1245.66	1289.43	950.12	398.92	462.24	488.60	0.39	0.00015	0.07378
540390	*Ssr3*	4389.37	5190.62	2063.27	1184.91	1158.31	1982.96	0.39	0.01056	0.16696
1690019	*Mest*	6712.69	6420.07	6332.16	1794.83	2574.71	3281.06	0.38	0.00063	0.08413
5570333	*LOC386144*	3095.62	2991.75	1248.65	678.60	1032.65	894.26	0.38	0.00813	0.15702
2480059	*Anxa5*	1860.18	1826.27	1097.72	649.96	544.17	558.57	0.38	0.00065	0.08413
7320152	*Ube2e3*	1295.03	1362.27	721.62	323.36	405.88	510.67	0.37	0.00227	0.11264
3140687	*Nrp*	8095.56	7848.63	3580.46	2966.49	1759.07	2164.00	0.37	0.00577	0.13838
4640338	*Klf7*	6815.14	6440.30	2119.51	1837.55	1362.56	1775.95	0.36	0.01521	0.18700
4900025	*LOC386360*	2674.01	2821.67	818.70	614.92	692.06	641.81	0.35	0.01562	0.18903
2690435	*Peg3*	9670.34	9364.16	5634.74	2278.11	2916.39	3233.71	0.35	0.00069	0.08413
2940047	*C630024B01Rik*	3770.39	4454.55	2341.05	905.09	1403.51	1277.33	0.35	0.00125	0.09486
2490274	*3010031K01Rik*	1832.88	1997.96	1592.41	554.77	1193.85	352.82	0.34	0.00843	0.15815
1050095	*Upp1*	2688.46	3011.33	1175.38	522.09	862.75	835.59	0.34	0.00614	0.14188
160519	*Tmem65*	2148.18	2243.17	1723.06	640.14			0.34	0.00004	0.06115
7610433	*Nsfl1c*	2443.26	2479.40	1029.14	289.11	604.30	1394.90	0.34	0.03952	0.25563
610092	*Grm6*	1041.87	1021.59	538.14	234.23	245.66	386.25	0.34	0.00213	0.10902

3890008	*E230020D15Rik*	3104.34	3249.09	905.42	690.95	703.45	695.84	0.33	0.01398	0.17957
5360367	*mtDNA_COXIII*	6692.16	7230.98	1772.64	1607.45	1076.52	1576.09	0.32	0.01915	0.20497
4060521	*Xist*	2281.13	2399.39	1088.77	471.60	543.83	684.85	0.31	0.00157	0.10062
5290523	*LOC280097*	1291.91	1057.60	451.94	261.24	258.45	260.97	0.31	0.00302	0.11416
5900392	*Xist*	3412.69	3236.13	1414.96	559.75	637.74	976.16	0.28	0.00240	0.11289
3520240	*Rn18s*	7124.23	5906.61	1959.66	495.18	1499.32	2077.42	0.27	0.02537	0.22570
630241	*LOC386288*	2382.44	2089.66	555.33	291.29	321.20	330.88	0.22	0.00526	0.13540
630519	*Mid1*	4744.18	4606.56	1153.44	1641.52	394.87	288.64	0.20	0.02222	0.21524
5260431	*LOC100043402*	3799.46	3167.20	923.10	280.66	466.51	480.63	0.18	0.00284	0.11416
4220386	*LOC100041388*	21340.58	19921.24	6750.41	1897.98	2517.94	2617.46	0.16	0.00072	0.08413
2750066	*Rn18s*	4838.85	3979.86	1234.09	256.45	565.87	608.15	0.15	0.00257	0.11406
6330047	*LOC386112*	8759.81	8220.00	2278.11	653.75	817.62	851.12	0.14	0.00099	0.09054
650221	*LOC385923*	10686.55	9996.04	1148.23	739.96	644.95	623.63	0.13	0.01050	0.16671
1230494	*LOC386199*	7713.92	6461.29	1345.22	329.65	595.85	642.00	0.12	0.00308	0.11416
4780753	*LOC386330*	13276.58	14333.16	2362.85	706.00	1063.78	1116.09	0.12	0.00340	0.11945

Supplemental Figures

Figure S1

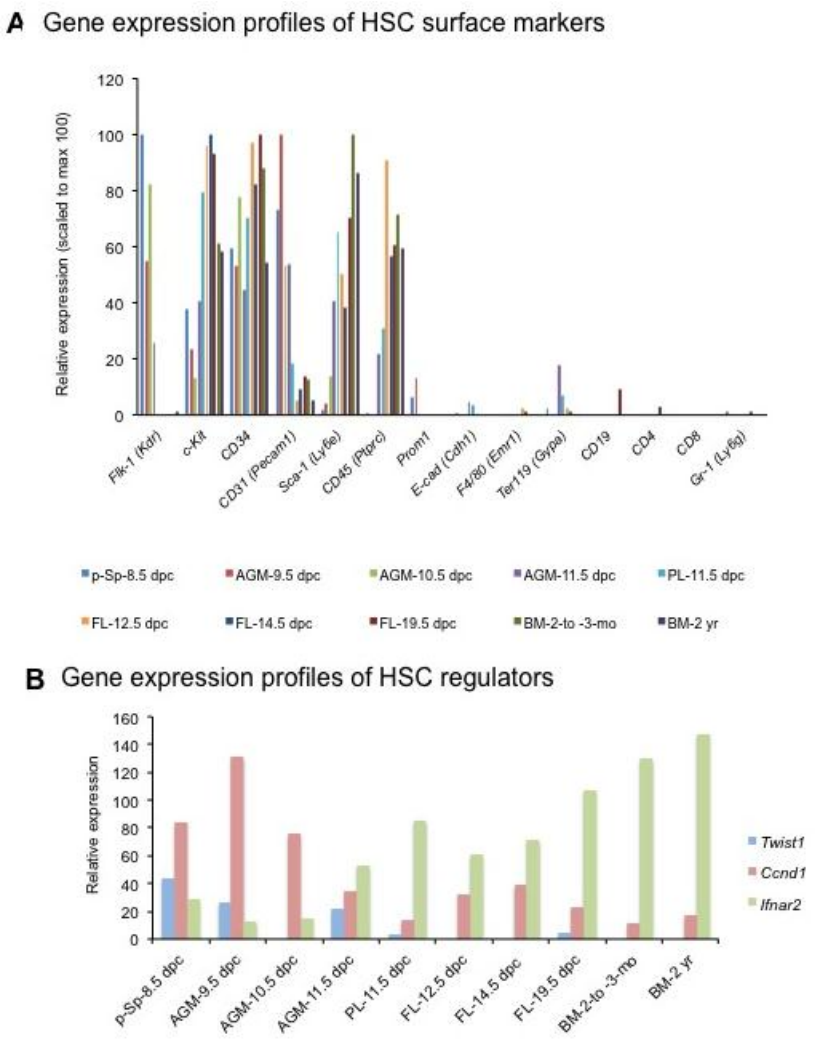

FIG. S1. (A) Expression profiles of genes encoding HSC surface markers (Flk-1, c-Kit, CD31, CD34 and Sca-1) and lineage markers (E-cad, F4/80, Gr-1, CD4, CD8, Ter119 and CD19) over the course of HSC development. The X-axis shows gene names, and the Y-axis their relative expression. (B) Expression profile of genes (*Twist1*, *Ccnd1* and *Ifnar2*) encoding HSC regulators during HSC development. The X-axis shows the 10 samples obtained at different sites at different stages, and the Y-axis indicates relative expression of each gene.